Russian Chemical Reviews **78** (12) 1153 – 1171 (2009) © 2009 Russian Academy of Sciences and Turpion Ltd

DOI 10.1070/RC2009v078n12ABEH004072

Electronic structure and chemical properties of superheavy elements

V Pershina

Contents

I.	Introduction	1153
II.	Relativistic and QED effects on the atomic electron shells of superheavy elements	1153
III.	Relativistic quantum chemical methods	1155
IV.	Atomic properties	1157
V.	Electronic structure and properties of gaseous compounds	1159
VI.	Complexation and extraction	1168
VII.	Conclusion	1169

Abstract. Relativistic electronic structure calculations of superheavy elements ($Z \geqslant 104$) are analyzed. Preference is given to those related to experimental research. The role of relativistic effects is discussed. The bibliography includes 164 references.

I. Introduction

Studies on the chemical properties of superheavy elements (SHE) and their compounds are a key avenue of chemical research, aimed at finding analogies between the properties of new elements and their lighter neighbours in the groups of the chemical elements and, eventually, proving their position in the periodic table. Nowadays, fourteen transactinide elements with Z from 104 to 118 with the exception of $Z = 117$, are known.[1,2] These elements are located at the bottom of the periodic table, their nuclei are extremely unstable and the electron shells are influenced by strong relativistic effects.[3] This makes experimental and theoretical research in the field very exciting and challenging.

Due to the instability of isotopes of these elements and low production rates, experimental chemical investigations are very complicated and require the development of special techniques to study the macrochemical properties on the basis of single-atom events.[4] At present, only the volatility in the gas phase and complexation in aqueous solutions can be studied using chromatography separation techniques.[5–11] The assumptions of the chemical composition of compounds of the new elements can only be made by assessing similarity in behaviour with the lighter homologues in the chemical groups. The spectroscopic properties can presently not be measured at all. Thus, theoretical investigations of SHE are extremely important, often being the only source of useful chemical information. Finally, it is just theory that can reveal the influence of relativistic effects on the chemical properties and experimental behaviour of SHE because the magnitude of relativistic effects can be determined only by comparing the observed behaviour with that predicted from relativistic and non-relativistic calculations.

Theoretical chemical research on heavy elements is nontrivial. To reliably predict the properties and experimental behaviour of the new elements, it should be based on the most accurate relativistic atomic and molecular calculations. It also requires the development of specific methods for the determination of quantities that cannot be predicted in a straightforward way using quantum chemical calculations.

Recent progress in relativistic quantum theory, computational algorithms and computer techniques have made very accurate calculations of the properties of the heavy elements and SHE possible. In this review, we will highlight recent advances in this field, with emphasis placed on the studies concerned with prediction of experimental behaviour of SHE. Particular attention will be paid to the influence of relativistic effects on the chemical properties and to trends in the periodic table.

Earlier reviews of quantum chemical calculations of transactinides and their compounds can be found in the literature.[12–19] A modern version of the periodic table of the elements is shown in Fig. 1.

II. Relativistic and QED effects on the atomic electron shells of superheavy elements

The relativistic mass increase is given by

$$m = \frac{m_0}{\left[1 - (v/c)^2\right]^{1/2}}, \qquad (1)$$

where m_0 is the rest mass and v is the velocity of an electron. As a consequence, the effective Bohr radius

V Pershina Gesellschaft für Schwerionenforschung (GSI), Helmholtzzentrum für Schwerionenforschung Gmbh, Planck-Str. 1, 64291 Darmstadt, Deutschland. Fax (49-061) 5971 34 63, tel. (49-061) 5971 24 61, e-mail: V.Pershina@gsi.de

Received 29 April 2009
Uspekhi Khimii **78** (12) 1243 – 1262 (2009)

1																	18
1 H	2											13	14	15	16	17	2 He
3 Li	4 Be											5 B	6 C	7 N	8 O	9 F	10 Ne
11 Na	12 Mg	3	4	5	6	7	8	9	10	11	12	13 Al	14 Si	15 P	16 S	17 Cl	18 Ar
19 K	20 Ca	21 Sc	22 Ti	23 V	24 Cr	25 Mn	26 Fe	27 Co	28 Ni	29 Cu	30 Zn	31 Ga	32 Ge	33 As	34 Se	35 Br	36 Kr
37 Rb	38 Sr	39 Y	40 Zr	41 Nb	42 Mo	43 Tc	44 Ru	45 Rh	46 Pd	47 Ag	48 Cd	49 In	50 Sn	51 Sb	52 Te	53 I	54 Xe
54 Cs	55 Ba	57 La	72 Hf	73 Ta	74 W	75 Re	76 Os	77 Ir	78 Pt	79 Au	80 Hg	81 Tl	82 Pb	83 Bi	84 Po	85 At	86 Rn
87 Fr	88 Ra	89 Ac	104 Rf	105 Db	106 Sg	107 Bh	108 Hs	109 Mt	110 Ds	111 Rg	112 –	113 –	114 –	115 –	116 –	(117)	118 –
(119)	(120)	(121)															

Lanthanides	58 Ce	59 Pr	60 Nd	61 Pm	62 Sm	63 Eu	64 Gd	65 Tb	66 Dy	67 Ho	68 Er	69 Tm	70 Yb	71 Lu
Actinides	90 Th	91 Pa	92 U	93 Np	94 Pu	95 Am	96 Cm	97 Bk	98 Cf	99 Es	100 Fm	101 Md	102 No	103 Lr
Superactinides	(122)	(123)	(124)	(125)	(126)									(153)

Figure 1. The Periodic Table of the elements as of 2009.[18]

$$a_B = \frac{\hbar^2}{mc^2} = a_B^0\sqrt{1-(v/c)^2}\,, \qquad (2)$$

where a_B^0 is the non-relativistic Bohr radius, rapidly decreases inner electrons. The contraction and stabilization of the s and $p_{1/2}$ orbitals is a consequence of this direct relativistic effect, and originates from the inner K and L shell region. The second, indirect, relativistic effect is the destabilization and expansion of the $p_{3/2}$, d and f AOs, screened from the nuclei by the s and $p_{1/2}$ AOs. The third effect is the spin-orbit splitting of the AOs with $l > 0$. All the three effects change approximately as Z^2 for valence shells down a column of the periodic table. For the heaviest elements, the magnitudes of these effects are very large. An example of relativistic stabilization of the ns and $np_{1/2}$ AOs and the spin-orbit splitting of the np AOs of the Group 14 elements is shown in Fig. 2. The latter effect amounts to 50 eV for element 164.[3] Figure 3 shows the relativistic contraction of the 7s AO in Db

$$\Delta_R\langle r\rangle_{7s} = \frac{\langle r\rangle_{nr} - \langle r\rangle_{rel}}{\langle r\rangle_{nr}} \times 100 = 25\%,$$

where $\langle r\rangle_{nr}$ and $\langle r\rangle_{rel}$ is the averaged relativistic and non-relativistic radius, respectively.

The relativistic contraction and stabilization of the ns AO reaches its maximum in the seventh row at element 112 (Fig. 4).[14] The shift of the maximum in the seventh row to element 112 compared to the sixth row (at gold) is due to the

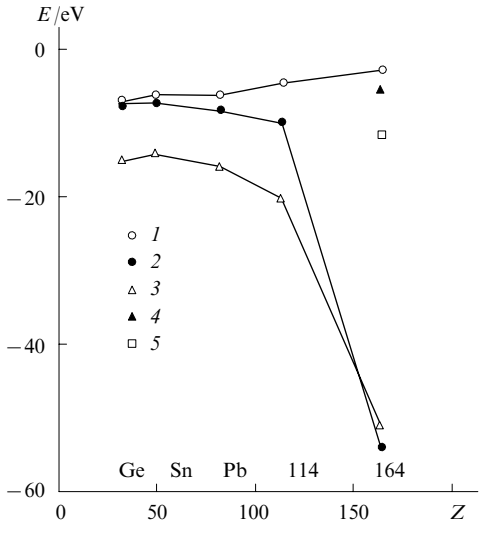


Figure 2. Energy eigenvalues of the valence electrons of Group 14 elements in the sp^2-configuration.[3,18] Obtained in the Dirac–Slater (DS) approximation; (*1*) $np_{3/2}$, (*2*) $np_{1/2}$, (*3*) $ns_{1/2}$, (*4*) $9s_{1/2}$, (*5*) $8d_{3/2}$.

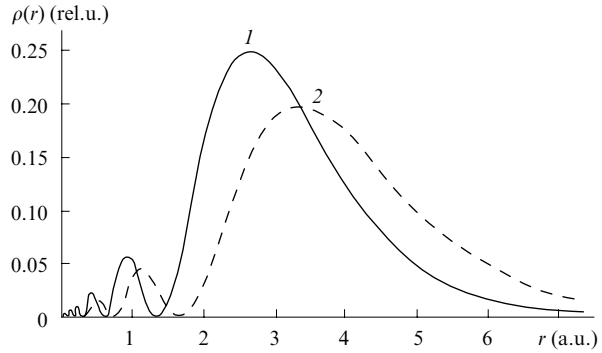


Figure 3. Relativistic (*1*) and nonrelativistic (*2*) radial distribution of the 7s valence electrons in element 105 (Db).[16]

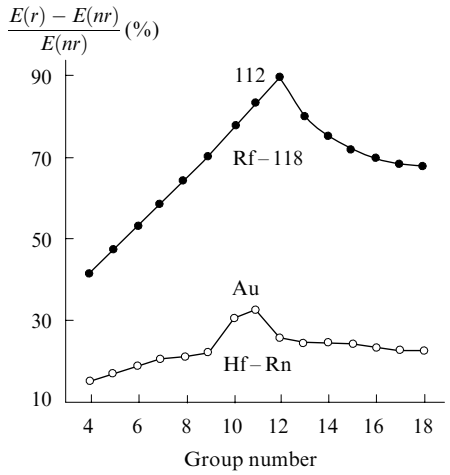


Figure 4. Relativistic stabilization of the 6s and 7s orbitals in the sixth and seventh row elements (obtained in the Dirac–Fock approximation).[14,18]

fact that in both elements 111 and 112 the ground-state electronic configuration is $d^q s^2$, while the electronic configuration changes from Au($d^{10}s^1$) to Hg($d^{10}s^2$).

Relativistic destabilization of the 6d AOs along with the stabilization of the 7s AOs results in inversion of the 7s and $6d_{5/2}$ energy levels of element 112, so that the first ionized electron is $6d_{5/2}$ rather than 7s as in mercury (Fig. 5). (An inversion of the 7s and 6d levels in the seventh raw begins already at hassium). Figure 5 shows some trends in the relativistic and non-relativistic energies of the ns AOs (the same is valid for the $np_{1/2}$ AOs). These trends become opposite as one proceeds from the sixth to seventh row of the periodic table, which will result in opposite trends in the relativistic and non-relativistic properties governed by those AOs.

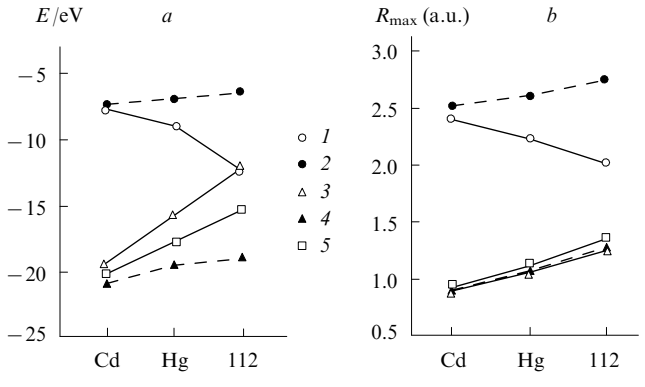


Figure 5. Relativistic DF[19] (solid lines) and non-relativistic Hartree–Fock (HF, dashed lines) AO energies (*a*) and radii of the maximum electron density (*b*) of the valence AO of Group 12 elements.[18] $ns_{1/2}$ (*1*), ns^{nr} (*2*), $(n-1)d_{5/2}$ (*3*), $(n-1)d^{nr}$ (*4*) and $(n-1)d_{3/2}$ (*5*).

In the 7p series of the elements, the stabilization of the $7s^2$ electron pair is so large that it becomes practically an inert pair. The stabilization of the $7p_{1/2}$ AO and the spin-orbit splitting of the 7p AOs is also very large for these elements; the latter parameter reaches a value of 11.8 eV for element 118. For the heavier elements, relativistic effects on their valence orbitals are even more pronounced and can lead to the onset of properties which are very different from those of the lighter homologues. Relativistic effects on the properties of elements up to $Z = 172$ are discussed in Ref. 3.

The Breit effects on the valence orbital energies and ionization potentials of the SHE are small, being, *e.g.*, only 0.02 eV for element 121.[20] They can, however, reach a few per cent for the fine-structure level splitting in the 7p elements and are of the order of correlation effects there. For element 121, the Breit effects can be as large as 0.1 eV for the transition energies between states including f AOs.

Quantum electrodynamic (QED) effects are known to be very important for inner shells (*e.g.*, in accurate calculations of X-ray spectra[21]). For SHE, the QED contribution to the orbital energy will be the second important one after the relativistic contribution. For instance, it was found that for element 118 the QED effects (self-energy and vacuum polarization corrections to the binding energy of the 8s electron) reduce the electron affinity (EA) by 9%.[22]

III. Relativistic quantum chemical methods

The most appropriate quantum chemical methods for electronic structure calculations of SHE are those which include both relativistic and correlation effects at the highest level of theory.[20]

1. Atomic codes

The highest theoretical level for the many-body methods is the Dirac–Coulomb–Breit (DCB) Hamiltonian

$$h_{\mathrm{DCB}} = h_{\mathrm{DC}} + \sum_{i<j} B_{ij}\,, \tag{3}$$

where

$$h_{\mathrm{DC}} = \sum_i [c\alpha_i \rho_i + (\beta_i - 1)] + V^n + \sum_{i<j} \frac{1}{r_{if}}\,, \tag{4}$$

α_i and β_i are the Dirac matrices, V^n is the nuclear potential, $1/r_{ij}$ is the operator of instantaneous Coulomb interaction between ith and jth electrons, and B_{ij} is the Breit operator

$$B_{ij} = -\frac{1}{2}\left[(\alpha_i \alpha_j) r_{ij}^{-1} + (\alpha_i \mathbf{r}_{ij})(\alpha_j \mathbf{r}_{ij}) r_{ij}^{-3}\right]. \tag{5}$$

The term V^n includes the effect of the finite nuclear size, while some finer effects, *e.g.*, QED ones, can be added to h_{DCB} perturbatively. The DCB Hamiltonian in this form includes all effects up to the second order in the fine-structure constant α.

Correlation effects can be taken into account by the configuration interaction (CI), many-body perturbation theory (MBPT) and, at the highest level of theory, using the coupled cluster with inclusion of single and double excitations (CCSD) technique.

The Fock Space (FS) DCB CC method[23] is presently the most powerful method which can be applied in studies of SHE. The method has an accuracy of few hundredths of an eV for excitation energies in heavy elements, because it takes into account most of the dynamic correlation effects (states with high l). It was used to treat atoms of many transactinides with Z from 104 to 122. Due to the present limitation of the FS CCSD approach [treatment of electronic configurations with more than two electrons (holes) beyond the closed shell is impossible], calculations for the middle of the 6d-series (elements 105–110) have not yet

been performed. Further developments will allow one to remove this limitation.[23]

The DC (Dirac – Coulomb) FS CCSD(T) method incorporated into the DIRAC program[24] has a slightly lower accuracy than the DCB FS CC approach. It was used to calculate the properties of elements with Z from 112 to 118.

A convenient tool for treatment of many-electron open-shell systems is the multiconfigurational Dirac – Fock (MCDF) method.[25,26] Based on the CI technique, it accounts for most of the correlation effects while retaining a relatively small number of configurations. It ignores, however, dynamic correlation effects, which makes it less accurate than the DC(B) CCSD technique. It was used for calculations of the electronic states of elements 104 – 108, 112 – 114 and heavier elements.[27–32] Electronic states of element 114 were also calculated using the relativistic multiconfigurational self-consistent field complete active space MCSCF (CASMCSCF) CI method.[33,34] Also, many atomic calculations were performed using molecular methods (see below). By and large, the results of modern accurate atomic calculations agree rather well with earlier predictions made using the DF and DS methods,[3] where the calculated energy terms were corrected taking into account the differences with experiment for the lighter homologues.

2. Molecular methods

Ideally, the most accurate method for solving the many-electron Eqn (3) should be free from approximation. Nevertheless, the problems of electron correlation and proper basis sets make *ab initio* DF methods of limited use in studies of heavy-element systems. Most of the molecular *ab initio* DF methods account for the correlation using the CI, Møller – Plesset (MP2), or CCSD(T) techniques.[35,36] These methods are still too time-consuming and not sufficiently economic to be applied to SHE-containing systems, especially, to large molecules and complexes studied experimentally, in a routine manner. Mostly small molecules, like hydrides or fluorides, were studied at this level of theory.[37–47]

Effective core potentials (ECP) were successfully used in studies of transactinide compounds. The energy-adjusted, or Stuttgart, pseudopotentials (PP)[48] and the relativistic ECP (RECP)[49] were used to calculate the electronic structures and properties of compounds of elements 111 – 114.[39,40,50–53] Calculations were performed with inclusion of relativistic (HF, spin-average RECP, AREP, AREP + SO) and correlation [MP2, CCSD(T)] effects in different manner and revealed the influence of these effects on the properties of chemically interesting molecules and complexes.

The RECP methods with inclusion of correlation effects at the MP2, complete active space MSCF (CAS-MCSCF) and CCSD(T) levels of theory were used for calculations of a number of gaseous chlorides and oxychlorides of elements from rutherfordium to seaborgium, as well as for some hydrides and fluorides of the 7p elements including element 118.[54–64] The RECP parameters were published by Nash.[65] Generalized RECP parameters accounting for Breit effects were developed for elements 112 – 114.[66]

The density functional theory (DFT) is most widely applied to transactinide compounds and to complexes in solutions and in the solid state. Due to overall simplicity and efficiency of computational algorithms, the DFT methods are most appropriate for treating chemically interesting large systems, adsorption processes, solids and solutions. (For instance, for a system of N atoms the DFT computing time increases as N_{at}^2 or N_{at}^3, while as $\exp(N_{\mathrm{at}})$ in traditional methods). The accuracy of the DFT methods depends on the correct choice of the exchange – correlation potential.[67,68]

The Dirac – Slater Discrete Variation (DS-DV) method[69,70] was extensively used in the past for calculations of the ground-state properties of transactinide compounds (see review[12]). Although the technique was inaccurate with respect to binding energies, it allowed one to make reliable predictions of ionization energies and the character of chemical bonding. The introduction of the relativistic generalized gradient approximation (RGGA) for the exchange – correlation potential and improvement in the integration scheme and basis set technique[71] made it possible to perform accurate calculations of binding energies and geometry optimization. The most recent version used nowadays for transactinide compounds is the four-component 4*c*-DFT combined with the non-collinear spin-polarized formalism,[72] which thus permits treatment of open-shell system. (The collinear approximation is also implemented.) The method uses numerical wave functions. The basis set optimization procedure is described in Ref. 72. The method was developed for very large systems, *e.g.*, clusters with more than hundred atoms and is therefore suitable for treatment of adsorption process and complexation. The possibility to treat a large number of atoms economically is achieved using the embedded cluster procedure (Fig. 6).[73]

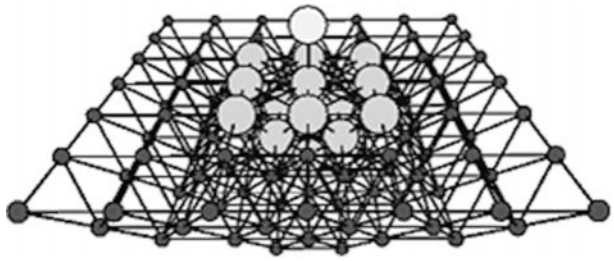


Figure 6. A system with embedded cluster $M - M_{14}$.[15]

A similar four-component method is the Beijing one (BDF).[74–77] It differs from the 4*c*-DFT method by the basis set technique, namely, four-component numerical atomic spinors obtained by finite-difference atomic calculations are used for cores, whereas the basis sets for valence spinors are combinations of numerical atomic spinors and kinetically balanced Slater-type functions. The results obtained for the same system, *e.g.*, $(114)_2$ using the 4*c*-DFT (Ref. 72) and BDF (Ref. 77) methods are very similar.

A number of quasi-relativistic approximations, *e.g.*, the 2*c*-DFT using the Douglas – Kroll (DK) approach[78] or the zero-order regular approximation (ZORA)[74] were used for calculations of heavy-element compounds as well. The SO ZORA calculations demonstrated very good agreement with the results of 4*c*-DFT method.[74] Some other methods, *e.g.*, the Douglas – Kroll – Hess technique,[79] were also used in calculations of simple SHE compounds.

IV. Atomic properties

1. Electronic configurations

The results of relativistic atomic calculations showed that relativistic stabilization of the 7s-AO of the seventh row elements results in the formation of the $7s^2$ electron pair in the ground state of the 6d and 7p elements, the $7s^26d^q$ and $7s^27p^q$, respectively. This is in contrast to the sixth row elements, where Pt and Au have different ground states, $5d^96s$ and $5d^{10}6s$, respectively (Table 1). The first excited states also differ for elements of these two series, *viz*., those of the 6d-elements contain the $7s^2$ electron pair.

Table 1. Ground-state electronic configurations of the 5d and 6d elements (Lu and Lr are also included).

Element	Configuration	Element	Configuration
Lu	$5d6s^2$	Lr	$7s^27p_{1/2}$
Hf	$5d^26s^2$	Rf	$6d^27s^2$
Ta	$5d^36s^2$	Db	$6d^37s^2$
W	$5d^46s^2$	Sg	$6d^47s^2$
Re	$5d^56s^2$	Bh	$6d^57s^2$
Os	$5d^66s^2$	Hs	$6d^67s^2$
Ir	$5d^76s^2$	Mt	$6d^77s^2$
Pt	$5d^96s$	Ds	$6d^87s^2$
Au	$5d^{10}6s$	Rg	$6d^97s^2$
Hg	$5d^{10}6s^2$	112	$6d^{10}7s^2$

It is remarkable that the controversy about the ground-state configurations of Lr and Rf was finally solved using the DCB FS CCSD method.[23] The DCB CCSD calculations[80] for lawrencium confirmed the MCDF $7s^27p_{1/2}$ state,[81] but rejected the MCDF $7s^27p6d$ configuration of rutherfordium[82,83] and gave the $7s^26d^2$ as ground state.[84] Such a high accuracy required the inclusion of correlation effects at a very high level of theory and augmentation of the basis set with the functions with $l = 6$. The DF calculations[19] for element 120 led to the $7p^68s^2$ relativistic ground state in contrast to the non-relativistic $7p^67d8s$ state.[14] According to the DCB CCSD calculations,[20] element 121 should have a $8s^28p_{1/2}$ ground state (in agreement with earlier DF results[3]) which is 0.4 eV lower in energy than the $8s^27d$ state (ground state of the lighter Group 3 homologues). Element 122 should have a $8s^27d8p$ state in contrast to the $7s^26d^2$ state of thorium.[85] This unusual configuration is due to relativistic stabilization of the $8p_{1/2}$ level. Recently,[86] DFT + QED calculations were performed for elements 121 – 131.

2. Ionization potentials, electron affinities and stability of oxidation states

The single-configuration DF ionization potentials (IP) of elements 104 – 166 are listed in Ref. 3. The MCDF calculated ionization potentials of elements from rutherfordium to hassium and elements 112 and 114, as well as the first ionization potentials of elements 113 – 119 are given in Refs 27 – 32, 83 and 87. The ionization potentials of elements 104, 111 – 115, 121 and 122 obtained from DCB CCSD calculations are available.[20,84,85,88–92] The ionization potentials of the sixth[93] and seventh row elements are shown in Fig. 7.

In elements 110 – 112, the first ionized electron is 6d in contrast to the lighter homologues Pt – Hg, although the ionization energies are higher. In elements 113 – 118, the first ionized electron is 7p, as expected. A large spin-orbit splitting of the 7p levels explains a drastic decrease in the ionization potential on going from element 114 to 115 due to the filling of the $7p_{3/2}$ shell for element 115, which is more destabilized than the $6p_{3/2}$ shell of Bi. The lower ionization potentials of elements 115 – 118 compared to those of their homologues Bi – Rn are also due to a large spin-orbit splitting of the 7p levels.

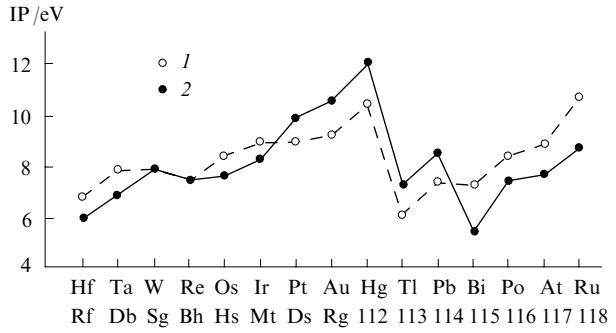


Figure 7. Ionization potentials of the sixth (*1*) and seventh (*2*) row elements.[18]
Experimental (*1*) and calculated (*2*) values.

Element 118 is expected to be the most electronegative in the group of the noble gases. Its outer 8s orbital is relativistically stabilized to such an extent that the electron affinity has a positive value of 0.058 eV according to DCB CCSD + QED calculations.[22,94] The inclusion of both relativistic and correlation effects was required to obtain this result. Similar calculations did not give a ^2S bound state for Rn^-. The ionization potential of element 118 calculated by the DC CCSD(T) method is 8.92 eV,[95] being the lowest among the Group 18 elements.

Relativistic stabilization of the $np_{1/2}$ electrons in Groups 13 and 14 is also responsible for a trend reversal in the decrease in ionization potential beyond In and Sn, respectively. Similarly, a reversal of the ionization potentials is observed from Sc to element 119 and from Ba to element 120 in Groups 1 and 2, respectively, due to the relativistic stabilization of the outer $ns_{1/2}$ electrons. According to DK CCSD calculations,[96,97] the ionization potential of element 119 increases from 3.31 to 4.53 eV due to relativistic effects. The decreasing trend in electron affinity in the group of alkali metals from Na to Cs is reversed starting with Cs due to the relativistic stabilization of the 7s (Fr) and 8s (119) electrons.

Owing to relativistic stabilization of the 8s electron, the electron affinity of element 119 is 662 meV (obtained from DCB CCSD calculations[98]), being the highest for Group 1 elements. The ionization potential of element 121 calculated by the same method is 4.45 eV and the electron affinity of element 121 is 0.57 eV, being the highest for Group 3 elements.[20] The DCB CCSD calculated ionization potential of element 122 is 5.59 eV (Ref. 85) (*cf*. 6.52 eV for thorium); this decrease is due to the relativistically stabilized $8p_{1/2}$ electron of element 122. The ionization potentials of heavier elements calculated in the DF and DS approximations can be found in Ref. 3.

The ionization potentials of internal conversion electrons (1s and 2s) for the elements 109, 112, 114, 116 and 118 are predicted to an accuracy of 10 eV using the DHF theory with inclusion of the QED and nuclear size effects.[21,99]

The relativistic stabilization of the 7s AOs and destabilization of the 6d AOs over the 6d elements should lead to increased stability of higher oxidation states, in agreement with the observed trends in groups of chemical elements. The MCDF calculations [27–29, 83] of the multiple ionization potentials of the elements from rutherfordium to hassium have indeed shown a decrease in the $(0 \rightarrow z^{+}_{max})$ ionization potential (Fig. 8). For the same reason, lower oxidation states of the early 6d elements will be unstable because stepwise ionization results in, *e.g.*, the $6d^2$ rather than $7s^2$ configurations of Db^{3+} or Sg^{4+}. Since the 6d orbitals of the 6d elements are destabilized relative to the $(n-1)$d orbitals of the 4d and 5d elements, Db^{3+} and Sg^{4+} will be less stable than Ta^{3+} and W^{4+}, respectively.[16]

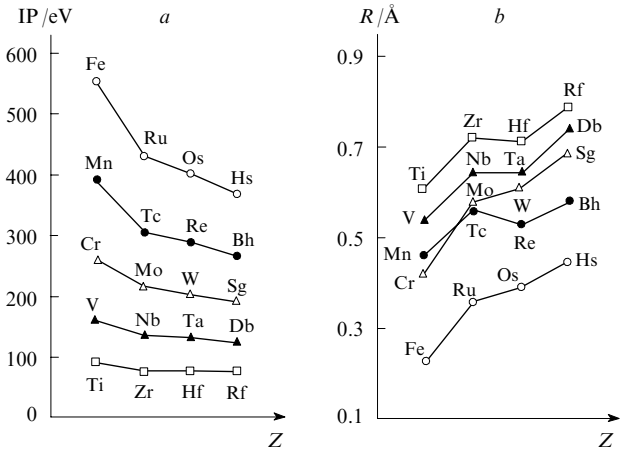


Figure 8. Multiple ionization potentials (*a*) and ionic radii (*b*) of elements in the maximum oxidation state.[16]
Ionization $0 \rightarrow 4+$, $0 \rightarrow 5+$, $0 \rightarrow 6+$, $0 \rightarrow 7+$ and $0 \rightarrow 8+$ for Group 4, Group 5, Group 6, Group 7 and Group 8 elements, respectively; the ionic radii were obtained from the MCDF calculations.[27–29, 83]

A trend to an increase in stability of the 3+ and 5+ oxidation states of roentgenium was also attributed to relativistic effects. Due to a relatively high electron affinity of roentgenium, the Rg^{1-} oxidation state may be accessible with appropriate ligands. The 4+ state of element 112 should be more stable than that of Au and Hg. The 0 oxidation state will dominate for element 112 due to its closed shell (electron affinity is zero [89]).

Strong relativistic stabilization of the $7s^2$ electrons and, therefore, a wide 7s–7p gap hindering hybridization is the reason for enhanced stability of lower oxidation states of the early 7p elements. Thus, the 1+ oxidation state will be more typical of element 113 than the 3+ state. Due to the relativistic stabilization of the $7p_{1/2}$ electrons the 2+ state should predominate over the 4+ state of element 114 to a greater extent compared to Pb. For elements 113 and 114, the 6d AOs should be still accessible for hybridization, thus making possible the formation of compounds of these elements in higher oxidation states, *e.g.*, $113F_5^-$ or $114F_6^{2-}$. Contrary to this, for elements 115–118 lower oxidation states should be more stable than those of the lighter homologues because the relativistically stabilized $7p_{1/2}$ AO is inaccessible for bonding. A typical oxidation state of element 115 should be 1+ due to the spin-orbit-destabilized $7p_{3/2}$ electron. The 3+ oxidation state should also be possible, while the 5+ oxidation state should not. For element 116, a decrease in stability of the 4+ oxidation state is expected due to a large spin-orbit splitting of the 7p levels, whereas the 2+ state should be more stable due to the presence of two destabilized $7p_{3/2}$ electrons. The 1+ and 3+ oxidation states should be the most typical of element 117, while the 5+ and 7+ oxidation states should be less typical. The 1− state of element 117 having one electron hole on the $7p_{3/2}$ AO should therefore be unusual (electron affinity of element 117 is the lowest in the group). For element 118, the 2+ and 4+ oxidation states are possible, while the 6+ oxidation state is less typical because of the strong binding of the $7p_{1/2}$ electrons. The oxidation states of heavier elements are discussed in Refs 3 and 14–18.

3. Atomic, ionic and covalent radii and polarizability

The atomic radii (AR) and ionic radii (IR) are defined by the maximum of the radial charge density (R_{max}) of the outer valence AO. The R_{max} values obtained from DF calculations for elements up to $Z = 120$ were tabulated by Desclaux.[19] Earlier discussions of the transactinide AR based on the results of the DF calculations are given in Ref. 3. The R_{max} values of elements from rutherfordium to hassium and their lighter homologues in groups in different oxidation states were obtained from MCDF calculations by Johnson, Fricke *et al.*[27–29, 83] In those works, the transactinide IR were obtained using a linear correlation between R_{max} and known IR [100] of elements in groups. The IR of elements from rutherfordium to hassium in the highest oxidation states are shown in Fig. 8. One can see that the IR of the 4d and 5d elements are almost equal due to the lanthanide contraction (of 0.020 Å) which is roughly 86% a nonrelativistic effect. The IR of transactinides are about 0.05 Å larger than those of the 5d elements due to an orbital expansion of the outer $6p_{3/2}$ orbitals responsible for the size of the ions. The IR of transactinides are, however, still smaller than those of actinides due to the actinide contraction (0.030 Å).

Atomic covalent radii (CR) for most of the elements of the periodic table including SHE to $Z = 118$ and 112 are given in Refs 101 and 102. They were determined from the calculated molecular bond lengths in various covalent compounds with double and triple bonds. The obtained single-bond CR for the Group 4–8 6d-elements are consistent with their IR. On the average, they are about 0.06 Å larger than the CR of the 5d elements (Fig. 9); the triple-bond CR

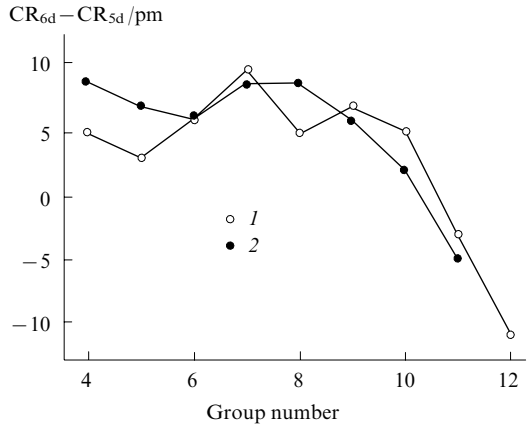


Figure 9. Differences in the lengths of single (*1*) and triple (*2*) bonds between the 6d and 5d elements.[18, 101, 102]

are on the average 0.08 Å larger. An important finding of those works is a decrease in the $(CR_{6d} - CR_{5d})$ difference starting from Group 9, which takes negative values for Group 11 and 12 elements as a result of relativistic bond contraction in compounds of elements 111 and 112.[102]

The static dipole polarizabilities α were calculated most accurately at the DC CCSD(T) level of theory for elements 112–118.[95, 103, 104] The effect of electron correlation on α was studied. According to the results obtained, α(112) should be the lowest for Group 12 elements due to the relativistic contraction of the outer 7s AO. The atomic polarizabilities of elements 113 and 114 are also lower than those of In and Tl, as well as Sn and Pb, respectively, which is due to the relativistic contraction of the outer $7p_{1/2}$ AO (see below). A reversal of the trends in α, AR and $R_{max}(np_{1/2})$ is observed in Groups 13 and 14 beyond In and Sn, respectively. For atoms of elements 115–118, α values are the largest in the respective groups† due to the largest $R_{max}(np_{3/2})$ values.[19] For instance, the α(118) value is the largest among all rare gases.[95] According to DK CCSD(T) calculations, the α(119) value is also relativistically decreased from 693.9 a.u. to 184.8 a.u. Relativistic calculations with improved basis set gave α = 165.98 a.u.[96]

V. Electronic structure and properties of gaseous compounds

1. Rutherfordium, dubnium, seaborgium, hassium

The 4*c*-DFT electronic structure calculations were performed for MF_4, MCl_4, MBr_4 (M = Zr, Hf, Rf); MCl_5, MBr_5, $MOCl_3$ (M = Nb, Ta, Db); MCl_6, MO_3, $MOCl_4$, MO_2Cl_2 and $M(CO)_6$ (M = Mo, W, Sg); MO_3Cl (M = Tc, Re, Bh); and MO_4 (M = Ru, Os, Hs) (see reviews [16, 17]). The results of RECP calculations for some Group 4–6 element halides and oxyhalides were also reported.[49, 54] Covalent compounds MX (X = H, N, B, C) were also considered.[101, 102]

According to the calculations, these transactinide compounds are in essence homologues of the lighter elements in respective groups and chemical bonding is determined by the valence $(n-1)$d AOs. An increase in stability of the maximum oxidation state and covalence of Group 4–8 elements was established and explained by relativistic effects.[105, 106] Figure 10 shows a relativistic decrease in the effective atomic charges of metals (Q_M) and an increase in the overlap population (OP) obtained from a Mulliken analysis of the electron density distribution in MCl_5 (M = V, Nb, Ta, Db).[105, 106] The changes observed are due to the relativistic stabilization of the ns and $np_{1/2}$ AOs with increasing *Z*. Trends in the non-relativistic values are opposite ongoing from Ta to Db.

The RECP CCSD(T) calculations of oxyhalides of Group 6 elements[54] without and with inclusion of spin-orbit coupling have shown that a slight decrease in the atomization energy (D_e) of compounds of the 6d elements compared to compounds of the 5d elements is due to the spin-orbit splitting of the 6d-AOs. A comparison of the average relativistic HF (AREP) and CCSD values also has demonstrated the importance of electron correlation effects responsible for about 65% of the D_e value of SgO_2Cl_2 (Table 2).

† A Borschevsky, V Pershina, E Eliav, U Kaldor, to be submitted.

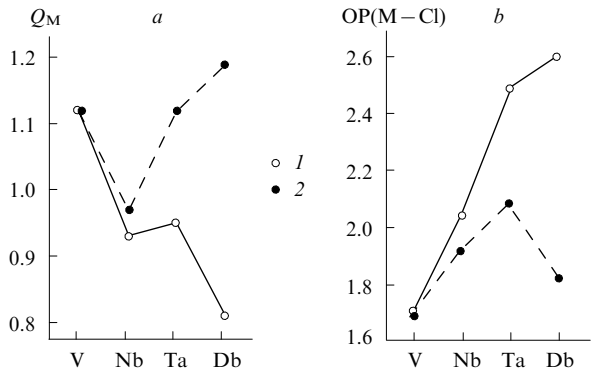


Figure 10. Effective charges (*a*) and overlap populations (*b*) for MCl_5 (M = V, Nb, Ta, Db) obtained in the relativistic (*1*) and non-relativistic (*2*) approximations.[13, 95]

Table 2. Atomization energies of WO_2Cl_2 and SgO_2Cl_2 calculated by the RECP method [54] with relativistic and electron correlation effects included in different manner. The additional SO effect is shown in the parentheses.

Molecule	HF (AREP)	MP2	CCSD	CCSD(T)	See [a]
WO_2Cl_2	11.7	24.4	20.9	22.1	23.5
SgO_2Cl_2	14.6 (−0.4)	24.8 (−1.3)	21.6 (−1.4)	22.5 (−1.6)	–

Note. Figures in parentheses denote the magnitude of additional spin-orbit effect. [a] Calculated using the Born–Haber cycle.

Both the 4*c*-DFT (Refs 107 and 108) and RECP (Ref. 54) calculations agreed that MO_2Cl_2 (M = Mo, W, Sg) is the most stable type of compounds among oxychlorides of Group 6 elements. Correspondingly, gas-phase chromatography experiments were conducted with dioxychlorides of these elements.[109, 110] $Sg(CO)_6$ was found to be very similar to $W(CO)_6$ and different from $U(CO)_6$.[111]

Geometry optimization calculations of various halides, oxyhalides, oxides and other compounds of Group 4–Group 8 elements have shown that the bond lengths (R_e) in compounds of the 4d and 5d elements are almost equal as a result of the lanthanide contraction, whereas R_e in compounds of the 6d elements are about 0.05–0.06 Å larger (see Figs 9 and 11) due to both the orbital and relativistic expansion of the $(n-1)$d AOs.

Based on the MO calculations, the adsorption enthalpies (ΔH_{ads}) of gaseous molecules on the surface of a quartz or silicon nitride (material for detectors) chromatography column needed for the design of gas-phase experiments were predicted (see Refs 15–18) using known adsorption models because first-principle quantum chemical calculations are still impossible. The models are based on the principle of molecule–slab interaction, where the interaction is subdivided into conventional types of long-range forces, *viz*., dipole–dipole, dipole–induced dipole and van der Waals (dispersion) ones. In particular, the adsorption energy of a molecule without dipole moment interacting with a dielectric surface is given by

$$E(x) = -\frac{3}{16}\left(\frac{\varepsilon-1}{\varepsilon+2}\right)\frac{\alpha_{mol}}{(1/IP_{slab} + 1/IP_{mol})x^3}, \qquad (6)$$

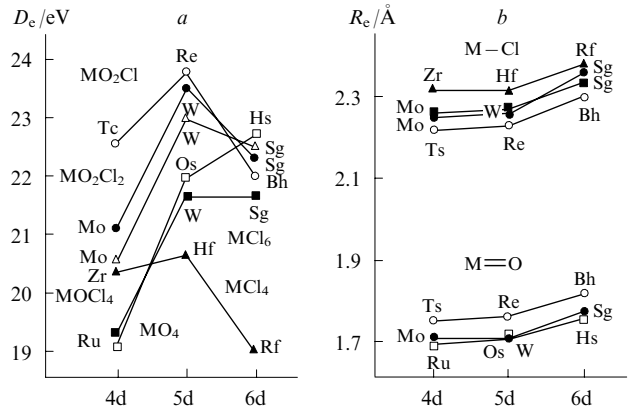


Figure 11. Atomization energies of (*a*) and bond lengths in (*b*) various gaseous compounds of Group 4–8 elements obtained from 4*c*-DFT (Refs 112–116) and RECP (Ref. 54) calculations.[16]

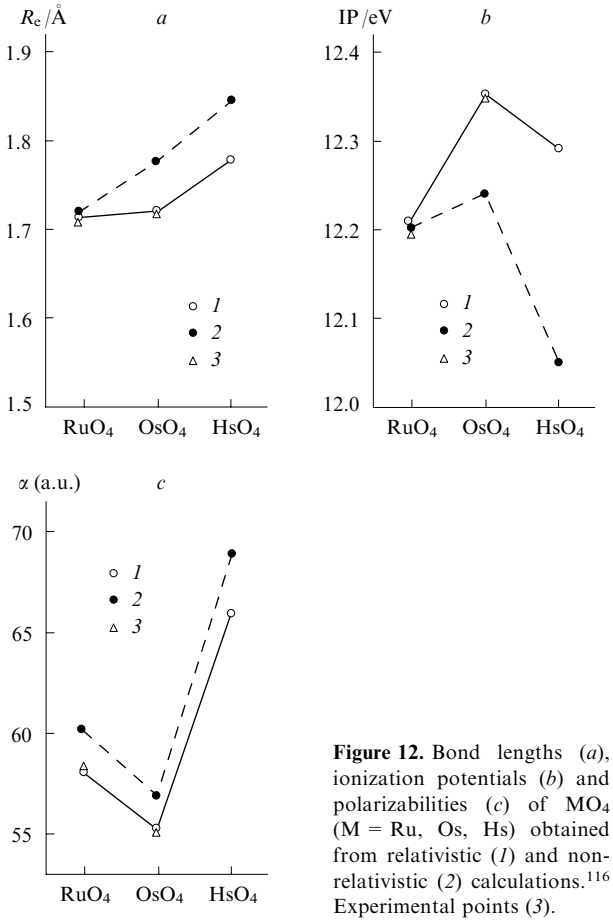


Figure 12. Bond lengths (*a*), ionization potentials (*b*) and polarizabilities (*c*) of MO_4 (M = Ru, Os, Hs) obtained from relativistic (*1*) and non-relativistic (*2*) calculations.[116] Experimental points (*3*).

where x is the distance between centre of the molecule and the surface atomic layer, the ε is the dielectric constant of the adsorbent material and IP is the ionization potential.[102] All molecular properties except x can be accurately calculated using relativistic codes, whereas x can only be evaluated (see Refs 114–116).

For instance, the $-\Delta H_{ads}$ values for BhO_3Cl (78.5 kJ mol^{-1}) and TcO_3Cl (48.2 kJ mol^{-1}) were determined using the adsorption models and accurately calculated molecular properties. Based on the results obtained, the following trend in volatility of oxychlorides of Group 7 elements was established:[113]

$$TcO_3Cl > ReO_3Cl > BhO_3Cl.$$

It was shown that this order of changes in the volatility is governed by the trend in the molecular dipole moments. Experimental study[117] of the volatility of oxychlorides of Group 7 elements gave $-\Delta H_{ads} = 75$ and 51 kJ mol^{-1} for BhO_3Cl and TcO_3Cl, respectively, which agrees with the theoretical values.

Prediction of the energy of weak interactions of MO_4 (M = Ru, Os, and Hs) molecules with an inert surface required calculations with a very high level of accuracy. To this end, the 4*c*-DFT calculations with extremely large basis sets were performed.[116] The obtained ionization potentials and α values of MO_4 (M = Ru, Os, Hs) are in perfect agreement with experimental values for the Ru and Os oxides. In this group of compounds, trends in these parameters are reversed, whereas R_e increases monotonically (Fig. 12). The trends were shown to be determined by the behaviour of the $(n-1)$d AOs of Group 8 elements. The $\Delta H_{ads}(MO_4)$ values for the MO_4 molecules on quartz were calculated from Eqn (6) using the IP and α values and the predicted trend in volatility of these compounds is as follows:

$$RuO_4 < OsO_4 > HsO_4.$$

Thermochromatography experiments revealed that HsO_4 is indeed about 6 kJ mol^{-1} stronger adsorbed on the silicon nitride surface of detectors than OsO_4.[118] The result obtained, $-\Delta H_{ads} = 46 \pm 2$ kJ mol^{-1}, is in excellent agreement with the theoretical value of 45.4 ± 1 kJ mol^{-1} (Ref. 116). This remarkable case demonstrates the importance of both exact calculations and statistically significant experiments. The non-relativistically calculated $-\Delta H_{ads}$ values of tetroxides of Group 8 elements revealed the same trends as corresponding relativistically calculated $-\Delta H_{ads}$ values because the orbital and relativistic effects on the $(n-1)$d-AOs act in the same direction. Relativistic effects on ΔH_{ads} values were shown to be negligible. There were some other attempts to interpret the volatility of HsO_4.[47, 119] However, calculations described in those studies have some drawbacks (for more detail, see Ref. 115).

2. Roentgenium

Similarly to AuH, roentgenium hydride RgH was used as a test system to compare the accuracy of various methods (DF, DK, PP and DFT). The results obtained are discussed in Refs 39, 40 and 101. A comparison of the spin-averaged relativistic pseudopotential (ARPP) with the nonrelativistic pseudopotential (NRPP) calculations showed that scalar relativistic effects double the D_e value, whereas the spin-orbit splitting of energy levels of the Rg atom (s^2d^9) decreases it by 0.7 eV [the (ARPP CCSD − SOPP CCSD) difference].[39, 40] Thus, the trend to an increase in D_e on going from AgH to AuH is reversed on going from AuH to RgH. The R_e(RgH) value should be similar to R_e(AuH).

Calculations in different approximations showed that the trend to an increase in the force constant k_e continues to RgH characterized by the largest k_e value among all known diatomic molecules. It was shown that the dipole moment μ_e decreases due to relativistic effects from AgH to AuH and then to RgH, thus indicating that RgH is more covalent and that roentgenium is a more electronegative element than gold. Large spin-orbit effects were found for R_e and k_e

(the corresponding estimates increase and decrease with inclusion of spin-orbit effects).[76]

The results of the 4*c*-BDF (Ref. 76) and 4*c*-DFT (Ref. 120) calculations for AuX and RgX (X = F, Cl, Br, O, Au, Rg) molecules indicate that the pattern of relativistic effects on their properties is similar to that for RgH, except for RgF and RgO where the spin-orbit splitting causes D_e to increase. However, the PP calculations[39] for RgH, RgLi and RgF showed that the spin-orbit effects are very small for R_e, but large for D_e (this parameter decreases in all cases, in contrast to the BDF calculations[76] for RgF). The scalar relativistic effects cause D_e(RgLi) to increase, however, D_e(RgF) to decrease. They cause R_e to decrease by about 0.4 Å in all cases. The singlet state of Rg_2 was found[120] to be more stable than the triplet state. It was established than the dissociation energy changes in the following order:

$$Au_2 > RgAu > Rg_2.$$

In order to study the stability of higher oxidation states of transactinides, the dissociation energies of the fluoride anions MF_4^- and MF_6^- (M = Cu, Ag, Au, Rg) in the decomposition reactions

$$MF_6^- \longrightarrow MF_4^- + F_2,$$

$$MF_4^- \longrightarrow MF_2^- + F_2$$

were calculated at the PP/MP2 and CCSD levels of theory.[50,53] It was shown that relativistic destabilization of the 6d AOs, which favours greater involvement of these AOs in chemical bonding, stabilizes higher oxidation states of roentgenium in high-coordination compounds. RgF_6^- was shown to be more stable than other fluorides. The spin-orbit coupling stabilizes the anions in the following order:

$$RgF_6^- > RgF_4^- > RgF_2^-.$$

This order is consistent with the relative involvement of the 6d electrons in the bonding for each type of compounds.

3. Element 112

It is known that Group 12 elements become more inert with increasing Z as a result of relativistic stabilization and contraction of the ns AOs. In particular, mercury is a liquid. For element 112, relativistic effects are expected to be even more pronounced.

Earlier, Pitzer[121] suggested that the very high energy (about 8.6 eV) of the $6d^{10}7s^2 \rightarrow 6d^{10}7s7p_{1/2}$ excitation of element 112 into the configuration of the metallic state will not be compensated by the energy gain of the metal–metal bond formation. The questions to the electronic structure theory were:

— is element 112 a metal in the solid state, or is it more like a solid noble gas?

— how volatile and reactive is element 112 atom as compared with mercury and radon and, especially, gold, which is used as a coating material for the surface of detectors in gas-phase chromatography experiments?

a. Atomic properties

The electronic structure of the atoms of mercury and element 112 was calculated in the framework of different approximations, namely, by the 4*c*-BDF method with the Perdew–Burke–Ernzerhof (PBE) functional and the PBE functional with self-interaction correction (PBESIC)‡ and at the QR-PP CCSD(T), ARPP CCSD(T),[52] ECP CCSD(T)[62] and DC(B) CCSD(T)[89,103] levels of theory. The best values for element 112 are the ionization potential equal to 11.07 eV [obtained from DBC CCSD(T) calculations[89]] and α = 27.64 a.u. [obtained from DC CCSD(T) calculations[103]]. The atomic properties of Group 12 elements calculated without and with inclusion of relativistic effects are shown in Fig. 13.

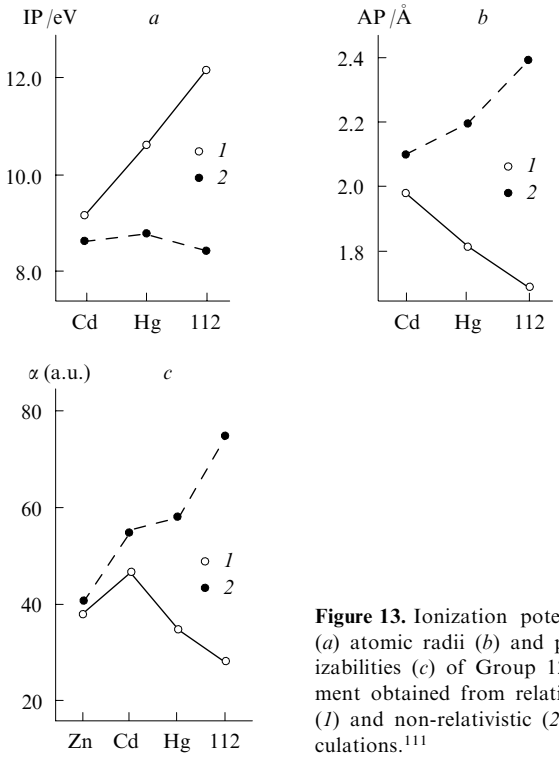


Figure 13. Ionization potentials (*a*) atomic radii (*b*) and polarizabilities (*c*) of Group 12 element obtained from relativistic (*1*) and non-relativistic (*2*) calculations.[111]

According to the calculations, element 112 has the highest ionization potential and the lowest polarizability among the Group 12 elements, which reflects the trends in AO energies and R_{max}, respectively (see Fig. 5). The relativistically calculated ionization potential of element 112 is 4 eV higher than that obtained from non-relativistic calculations, because the first electron detached is $6d_{5/2}$ in the former and the destabilized 7s in the latter case. The α(112) value equal to 45 a.u. is decreased due to the relativistic contraction of the 7s AO. For the same reason, the atomic radius of element 112 is relativistically contracted by 0.5 a.u., being the smallest for the Group 12 elements. The non-relativistic values have opposite trends beyond Cd (see Fig. 13).

b. Homonuclear dimers

The first step to treat a 'macroamount' of element 112 is to find out how strong element 112 can be bound to itself. To this end, calculations of the spectroscopic properties of Hg_2 and $(112)_2$ were performed using different methods including 4*c*-BDF PBE, ECP CCSD(T), QP-PP CCSD(T)‡ and 4*c*-DFT.[120,122] It was shown that the chemical bonding in $(112)_2$ is determined by both the 7s and 6d AOs is not of pure van der Waals type, as in Hg_2.[123] The results of both DFT and PP calculations agree on an increase in D_e by

‡ W Lin, M Dolg, P Schwerdtfeger. Unpublished results.

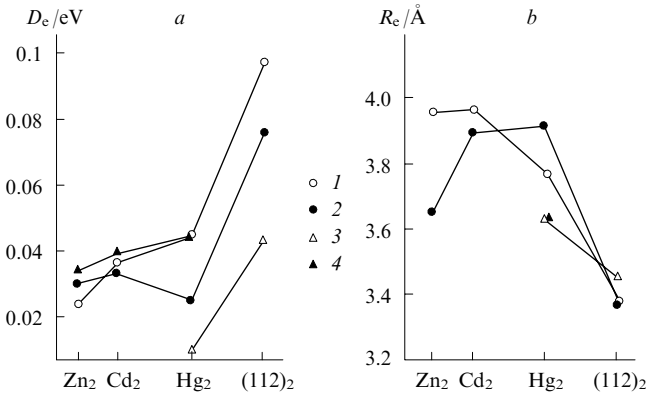


Figure 14. Dissociation energies (*a*) and bond lengths (*b*) in dimers of the Group 12 elements.[18]
Obtained from the QR PP CCSD(T) (*1*), 4*c*-BDF PBESIC (*2*) and 4*c*-DFT (*3*) calculations. Experimental points (*4*).

about 0.04 eV on going from Hg_2 to $(112)_2$ owing to shortening of the bond, in line with the condition $R_{max}[7s(112)] < R_{max}[6s(Hg)]$ (Fig. 14).

c. Solid state

Non-relativistic, scalar relativistic and 4*c*-relativistic LDA DFT band structure calculations[124] were performed for the solid state of element 112. It was found that element 112, similarly to Zn and Cd, prefers the *hcp* structure (*cf.* the *fcc* structure for Hg). Thus, structurally, element 112 should be different from its lighter homologue, Hg, and resemble solid noble gases. The cohesive energy of element 112 (1.13 eV, obtained from SR calculations) is higher than that of Hg (0.64 eV) and an order of magnitude higher than those of the solid noble gases. It was concluded that element 112 is most likely a semiconductor with a band gap of at least 0.2 eV. (The results of the LDA calculations were considered as a lower bound). In this sense, element 112 resembles the Group 12 metals rather than noble gases.

d. Adsorption on inert surfaces

Knowledge of the adsorption enthalpy of element 112 on inert surfaces such as quartz and ice (which can be formed below -80 °C in the chromatography column) is needed for designing gas-phase chromatography experiments. To this end, the ΔH_{ads} values of mercury, element 112 and radon on these materials were determined using the adsorption model [see Eqn (6)] and the calculated atomic properties.[103, 122] The results thus obtained ($-\Delta H_{ads} = 40.5$ kJ mol^{-1} for mercury on quartz and 25.2 kJ mol^{-1} for mercury on ice) are in good agreement with the experimental values of 42 ± 2 kJ mol^{-1} and 25.5 ± 2 kJ mol^{-1}, respectively.[125] The predictions for element 112 are $-\Delta H_{ads} = 43.2 \pm 0.2$ kJ mol^{-1} on quartz and $-\Delta H_{ads} = 26.3 \pm 0.1$ kJ mol^{-1} on ice. Thus, element 112 is expected to be deposited on ice in the thermochromatography column at slightly higher temperatures than mercury. The reverse was obtained from non-relativistic calculations.

A chemically important conclusion is that element 112 is bound by van der Waals forces stronger than Hg in the homonuclear dimer, in the solid state and in the adsorbed state on an inert surface due to the relativistic contraction of the 7s AO (see Fig. 5).

e. Heteronuclear dimers

As a first step of studies of the adsorption of mercury and element 112 on noble metal surfaces, 4*c*-DFT electronic structure calculations of HgM and 112M (M = Ag, Au, Pt, Pd, Cu) were performed.[122, 126] It was shown that bonding of element 112 with Au occurs primarily through the participation of the 7s AO of element 112, although the 6d AOs are also active (Fig. 15). It was found that the D_e(112Au) value is about 0.2 eV lower than D_e(HgAu) and that R_e(112Au) is larger than R_e(HgAu).

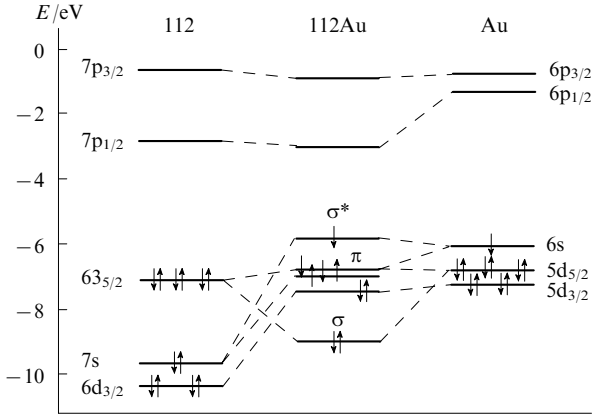


Figure 15. Bond formation (principal MOs) in the 112Au molecule.[18]

It was shown that relativistic effects cause D_e(HgAu) to increase by 0.13 eV and D_e(112Au) to decrease by about the same value (0.12 eV). The R_e decreases due to relativistic effects in both systems. Relativistic effects cause the vibrational frequencies (w_e) of each compound to increase, but this increase for 112Au is much smaller than for HgAu. Relativistic contraction of the 7s AOs is responsible for the decrease in both the ionic and covalent contributions to the bonding of element 112.[122]

e. Adsorption on gold clusters

Studies of adsorption of mercury and element 112 on a gold surface involved the 4*c*-DFT calculations of a 'metal atom–gold cluster' system.[122, 127–129] Since the structure of gold layers covering silicon detectors is unknown, two types of the ideal surface were considered, Au(100) and Au(111). They were simulated by clusters of various size containing up to more than 100 atoms.

The potential energy curves obtained from the calculations[129] of the embedded clusters $M-Au_nAu_m$ (M = Hg, element 112; $n_{max} = 36$ and $m = 156$) simulating the Au(100) surface are shown in Fig. 16. As can be seen, the binding energy (E_b) of element 112 with gold is 0.1–0.3 eV lower than with Hg depending on the geometry of the adsorption complex and the bridge position of the adsorbed atom should be preferred. Using the difference between the calculated ($E_b = 1.52$ eV) and experimental ($-\Delta H_{ads} = 1.03$ eV) values for mercury on gold,[130] one gets $-\Delta H_{ads}(112) = 0.65$ eV for element 112.[129]

The 4*c*-DFT calculations[131] for mercury and element 112 interacting with large gold clusters (up to $n = 120$)

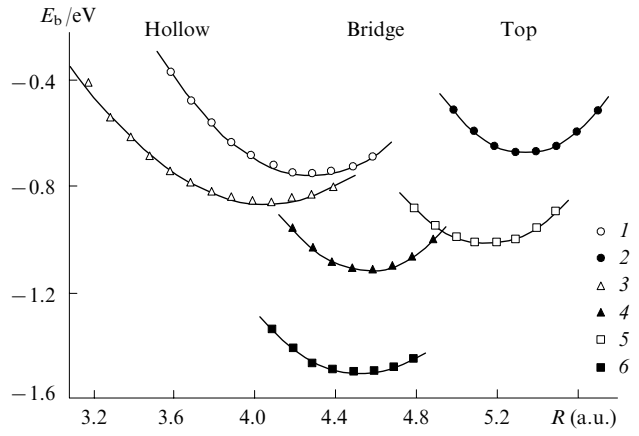


Figure 16. Potential energy curves obtained from the 4*c*-DFT calculations of the $M-Au_nAu_{156}$ clusters (M = Hg and element 112) simulating the Au(100) surface in three adsorption positions: top, hollow and bridge.[129]
$112Au_{29}$ (*1*), $112Au_{34}$ (*2*), $HgAu_{29}$ (*3*), $112Au_{36}$ (*4*), Hg/Au_{36} (*5*) and $HgAu_{36}$ (*6*).

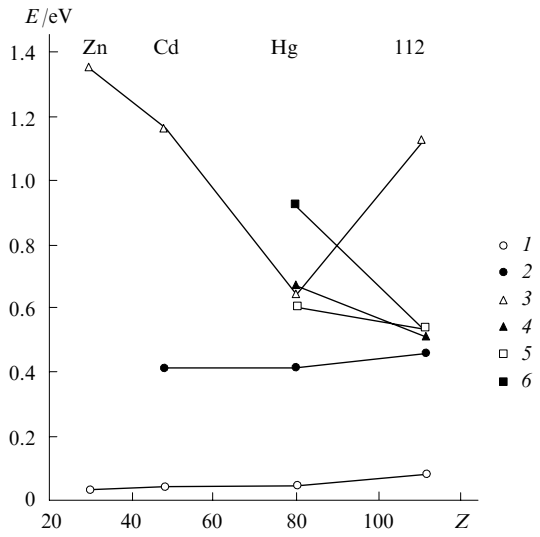


Figure 17. Binding energies of Group 12 elements (M = Zn, Cd, Hg, element 112) in different systems: $D_e(M_2)$ in the M_2 dimers (*1*), $-\Delta H_{ads}$ on quartz (*2*), $\Delta H_{sub}(M)$ of metals (*3*), $D_e(MAu)$ of the MAu dimers (*4*); $E_b(M-Au_n)$ (*5*); experimental $-\Delta H_{ads}$ on gold (*6*).
Solid and open symbols denote experimental points and results of calculations, respectively.[18]

simulating the Au(111) surface were also carried out. The results obtained showed the same relation between E_b(Hg) and E_b(112) as for the Au(100) surface, namely, element 112 is bound to gold about 0.1–0.2 eV weaker than mercury. By and large, E_b with the clusters simulating the Au(111) surface are lower than with the clusters simulating the Au(100) surface. The $E_b(112-Au_{94})$ value is 0.46 eV for the preferred bridge position on the Au(111) surface.

Predictions[129, 131] of the adsorption behaviour of element 112, mercury and radon are in perfect agreement with the experimental results. In the thermochromatography experiments,[132] a few decay chains attributed to an isotope of element 112 were observed at an adsorption temperature far from the temperature of the cold end (−180 °C) of the chromatography column where radon was adsorbed. (Mercury was deposited right at the beginning of the column with the warm-end temperature of 35 °C). Monte Carlo simulation using the observed adsorption temperatures gave $\Delta H_{ads}(112) = -52^{+4}_{-3}$ kJ mol^{-1}. Thus, experiments demonstrated that element 112 does not behave like radon, but apparently forms a chemical bond with gold, which is similar to (although weaker than) the Hg–Au bond. The predicted[131] E_b(112) value is in excellent agreement with the experimental ΔH_{ads}(112) value.

The RECP + DFT (SO corrected) calculations of the interaction of mercury and element 112 with small gold clusters ($n = 1-4$, 10) were also reported.[133] They by and large confirmed the results of the earlier 4*c*-DFT calculations,[122, 129] according to which element 112 should be bound to gold clusters weaker than mercury.

The influence of relativistic effects on the adsorption of mercury and element 112 on metal surfaces was investigated taking small 'metal atom–gold cluster' systems as examples. It was shown that relativistic effects cause the binding energy of element 112 with the gold clusters to decrease.

The binding energies of the Group 12 elements in various compounds are plotted *vs.* *Z* in Fig. 17.

f. Other compounds

The relativistic contraction of the 7s AO also manifests itself in the properties of other compounds of element 112. The relativistic bond length contraction similar to that of the Rg–H bond was found in $112H^+$; because of this, $R_e(112H^+)$ is the smallest among CdH^+, HgH^+ and $112H^+$.[51, 52, 62, 134, 135] Yet another interesting point is that, in contrast to the Group 11 element hydrides, the trend in the dissociation energies on going from CdH^+ to HgH^+ is continued with $112H^+$, *i.e.*,

$$D_e(CdH^+) < D_e(HgH^+) < D_e(112H^+),$$

but

$$D_e(AgH) < D_e(AuH) > D_e(RgH).$$

The reason for this difference is greater relativistic effects in $112H^+$ compared to RgH.

The results of PP CCSD(T) calculations of the energies of decomposition reactions of fluorides MF_2 and MF_4 (M = Zn, Cd, Hg, element 112)

$$MF_4 \longrightarrow MF_2 + F_2,$$

$$MF_2 \longrightarrow M + F_2$$

confirmed the increasing involvement of the 6d AOs of element 112 in chemical bonding and the enhanced stability of the 4+ oxidation state of the Group 12 elements.[52] A comparison with the results of non-relativistic calculations showed that this is a pure relativistic effect. The Mulliken population analysis for MF_2 and MF_4 (M = Hg and element 112) suggests that the 6d AOs of element 112 are involved in the bonding to a greater extent than the 5d AOs of mercury. It is believed that anions $112F_5^-$ and/or $112F_3^-$ can form in an appropriate polar solvent.[50, 52]

4. Element 113

The ground-state electronic configuration of element 113 is $7s^27p_{1/2}$. The 7s AO is relativistically stabilized to such an extent that it becomes inaccessible for bonding. The properties of element 113 will therefore be determined by the $7p_{1/2}$

AO, which is also relativistically stabilized and contracted; this does not favour the formation of strong covalent bonds.

The best calculated atomic properties of thallium and element 113 are given in Table 3. The trends to a decrease in the ionization potential and an increase in α for the Group 13 elements show a reversal starting with indium (Fig. 18). This is due to the strong contraction and stabilization of the outer $np_{1/2}$ AOs of these elements, with the strongest effect for element 113.

Table 3. Selected atomic properties of Tl and element 113.

Method	IP /eV	EA /eV	α (a.u.)	AR /Å	R_{vdW} /Å	Ref.
Thallium						
Calculations	6.108 [a]	0.40(5) [a]	51.29	1.38	1.90	104
Experiment	6.110	0.377(13)	51(7)	—		136, 137
Element 113						
Calculations	7.306 [a]	0.68(5) [a]	29.85	1.22	1.84 ± 0.01	104

[a] DCB RCC calculations.[90]

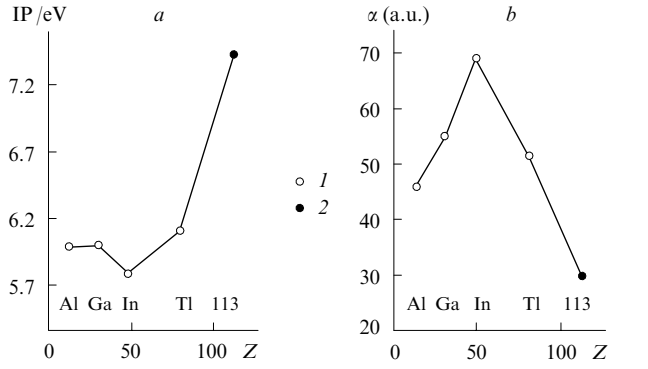


Figure 18. Ionization potentials (*a*) and polarizabilities (*b*) of the Group 13 elements. The data for element 113 were taken from the DC(B) FSCC calculations.[90,104]

The van der Waals radii, R_{vdW}, of thallium and element 113 were obtained using correlations of the known R_{vdW} values with $R_{max}(np_{1/2}\text{-AO})$ of Group 13 elements.[104] They also showed that the trend to an increase in R_{vdW} is reversed starting with In, so that $R_{vdW}(113)$ is the smallest among the Group 13 elements.

As the other 7p-elements, element 113 is expected to be volatile. The enthalpies of adsorption of Group 13 elements (from Al to element 113) on Teflon and polyethylene (PE) were predicted [104] using the adsorption model [see Eqn (6)] and the calculated atomic properties (see Table 3). The $-\Delta H_{ads}(113)$ values are 14 and 16 kJ mol^{-1} for adsorption on Teflon and PE respectively, being about 6 kJ mol^{-1} lower than the corresponding values for thallium. This makes it possible to separate element 113 from thallium using adsorption on these surfaces. The ΔH_{ads} values behave like α, *i.e.*, decrease starting with indium, so that the $\Delta H_{ads}(113)$ value is the smallest among the Group 13 elements. The extremely low enthalpy of adsorption on inert surfaces will enable easy transport of element 113 through the Teflon capillaries.

A very large spin-orbit splitting of the 7p levels is expected to influence the properties of compounds of the 7p elements from element 113 to element 118. The electronic structure of monohydrides (MH) of these elements and their lighter homologues in groups was calculated by the DFC, PP, RECP and 2*c*- and 4*c*-DFT methods (Refs 44, 55, 57–59, 64, 77, 120 and 138). The results obtained are shown in Fig. 19.

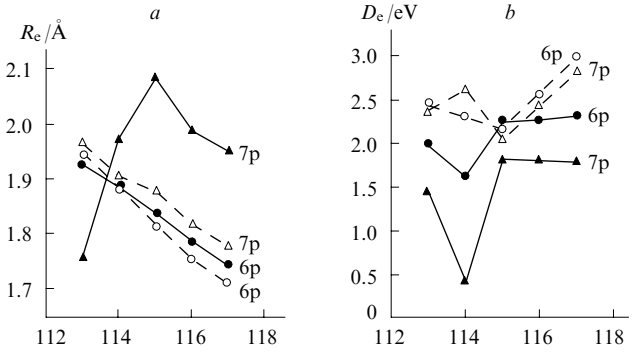


Figure 19. Bond lengths (*a*) and dissociation energies (*b*) of monohydrides of 6p (Tl–At) and 7p elements (element 113–element 117).[16,57–59,77]
The filled and open symbols denote the results of relativistic and non-relativistic calculations, respectively.

A large relativistic contraction of the $7p_{1/2}$ AO results in a large shortening of the 113–H bond. This was not found for other MH compounds because both the relativistically contracted $7p_{1/2}$ and expanded $7p_{3/2}$ AOs participate in the bonding in MH (M = 114–118); as expected, the contribution of the $7p_{1/2}$ AO gradually decreases along the series of the 7p elements. It was shown that $D_e(113H)$ increases by 0.9 eV due to the atomic spin-orbit splitting. A decreasing trend in D_e and k_e from BH to 113H was predicted.

The 2*c*-/4*c*-BDF and DF calculations [37,138] revealed a very low binding energy of $(113)_2$, namely, $D_e = 0.08$ eV for the BP potential and $D_e = 0.11$ eV for the PBESCC potential. The PP, DCB, RECP and 4*c*-DFT calculations (Refs 44, 50, 55 and 120) predicted an increase in R_e and μ_e from TlF to 113F and a decrease in these parameters from TlH to 113H. These different trends are explained by a more ionic nature of fluoride molecules.

The (113)(117) molecule was studied at the DF level of theory.[41] In this molecule, both the low-lying $7p_{1/2,1/2}(113)$ AOs and the destabilized $7p_{3/2,1/2}(117)$ AOs contribute to electron transfer to the atom of the Group 13 element. Instead of completing the valence p shell of the atom of the Group 17 element with a single electron of the atom of the Group 13 element, the electron density is displaced in the opposite direction, namely, the high-lying $7p_{3/2,1/2}$ shell of the 117 atom donates an electron to the low-lying $7p_{1/2,1/2}$ shell of the 113 atom. This results in reversal of the dipole direction and in a change in the sign of the dipole moment.

The results of the PP and RECP calculations [44,55,58] of $113X_3$ (X = H, F, Cl, Br, I) molecules showed that the involvement of the 6d AOs in bonding most probably leads to a T-shaped rather than trigonal planar geometric configuration of these molecules. This means that the valence shell

electron pair repulsion (VSERP) theory is inapplicable to SHE. Relativistic effects on the bond angles are assumed to be small; however, in the presence of Jahn–Teller distortions, they may significantly change the bond angles, as was shown for AtF_3.[139]

Calculations[44] predicted a stable high-coordination compound of $113F_6^-$ with a metal in the 5+ oxidation state, whereas the fluoride $113F_5$ will probably be unstable because the energy of the reaction

$$113F_5 \longrightarrow 113F_3 + F_2$$

is lower than -100 kJ mol^{-1}. The calculated energies of the decomposition reaction

$$MX_3 \longrightarrow MX + X_2$$

(M = B, Al, Ga, In, Tl, element 113)

suggest a decrease in the stability of the 3+ oxidation state of the elements in this group.

5. Element 114

The ground-state electronic configuration of element 114 is $7s^27p_{1/2}{}^2$. This quasi-closed shell is a result of strong relativistic stabilization of the $7p_{1/2}$ AO and a large spin-orbit splitting of the 7p AOs (see Fig. 2). As a consequence, the properties of element 114 and its compounds should be determined by the relativistically stabilized and contracted, doubly occupied $7p_{1/2}$ AO. Therefore, element 114 is expected to be rather inert and volatile. Its volatility can be studied by gas thermochromatography with gold covered detectors similarly to element 112.[132] Yet another method of studying the reactivity of element 114 is electrochemical deposition on various metal electrodes from acidic solutions.[9]

The most accurately calculated properties of element 114 and Pb are given in Table 4. The α(114) appeared to be the smallest for the Group 14 elements (with a reversal of the trend at Sn) due to the relativistic stabilization and contraction of the outer $7p_{1/2}$ AO (Fig. 20). It was shown that the spin-orbit coupling leads to a significant reduction of α(114) from 47.9 a.u. (scalar-relativistic DK calculations) to 31.5 a.u. (DC calculations).[140] The trend to a decrease in the ionization potentials of Group 14 elements is also reversed starting with tin, in line with the trend in α, so that the IP(114) is the largest (except for C). The van der Waals radii R_{vdW}(114) obtained using a correlation between the known R_{vdW} values of the Group 14 elements and corresponding $R_{max}(np_{1/2}\text{-AO})$ values show a similar reversal of the trend

Table 4. Selected atomic properties of Pb and element 114.

Method	IP /eV	α (a.u.)	AR /Å	R_{vdW} /Å	Ref.
Lead					
Calculations	7.349 [a]	46.96 [b]	3.40 [c]	4.06 [c]	103
Experiment	7.417	47.1 ± 7	3.40	4.16	136, 137, 140
Element 114					
Calculations	8.539 [a]	30.59 [b]	3.30 [c]	3.94 [c]	103

[a] Obtained from DCB CCSD calculations;[91] [b] obtained from DC CCSD(T) calculations; [c] determined using the correlation with $R_{max}(np_{1/2})$.

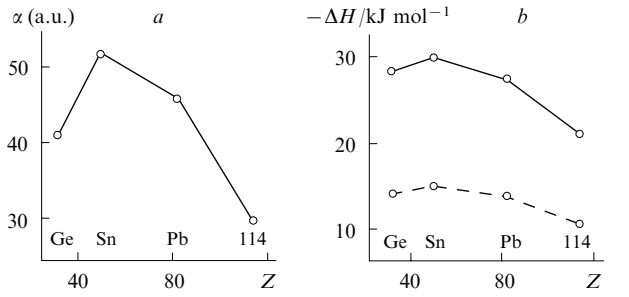


Figure 20. Polarizabilities (*a*) and enthalpies of adsorption (*b*) of Group 14 elements on polyethylene (solid line) and Teflon (dashed line) obtained from DC CCSD(T) calculations.[18,103]

starting with tin, so that R_{vdW}(114) is the smallest (except for C).[103]

The enthalpies of adsorption, ΔH_{ads}, of Group 14 elements on Teflon and PE were predicted[103] using the atomic properties (see Table 4) and the adsorption model [see Eqn (6)]. The calculated $-\Delta H_{ads}$ values for adsorption of lead and element 114 on PE are 27.34 and 20.97 kJ mol^{-1}, respectively (*cf.* 13.65 and 10.41 kJ mol^{-1} for adsorption on Teflon, respectively). The $-\Delta H_{ads}$ values exhibit the same reversal of the trend as the $R_{max}(np_{1/2})$ and α of the Group 14 elements (see Fig. 20). According to these values, element 114 should be well transported from the target chamber to a chemical setup through a Teflon capillary.

a. Homonuclear dimmers

The electronic structure of M_2 (M = Ge, Sn, Pb, element 114) species was calculated by the 4*c*-BDF,[77] 4*c*-DFT,[141] and RECP CCSD(T)[77] methods. According to calculations, the dimer $(114)_2$ is bound stronger than a typical van der Waals system; $D_e = 0.13$ (4*c*-DFT) and 0.07 eV [ECP CCSD(T)]. The D_e and R_e values for the Group 14 elements are shown in Fig. 21. The bonding in $(114)_2$ is stronger than in $(112)_2$, but much weaker than in Pb_2. A Mulliken population analysis indicates that both the $7p_{1/2}$ and $7p_{3/2}$ AO of element 114 participate in the

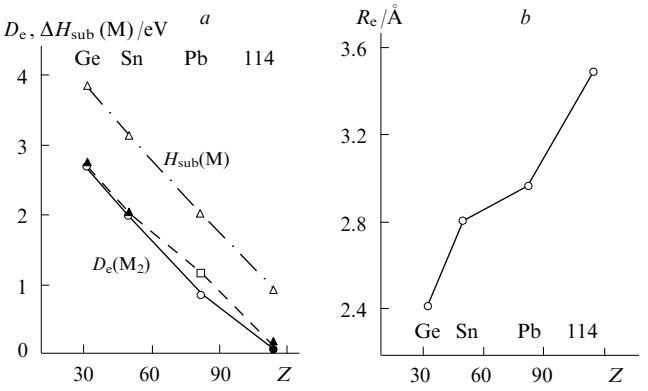


Figure 21. Dissociation energies of M_2 and sublimation enthalpies of metals (*a*) and calculated bond lengths in M_2 (M = Ge, Sn, Pb, element 114) dimers (*b*).[18]
(*a*) experimental data for Ge_2, Sn_2 and Pb_2 dimers (two points for Pb_2 represent two different experimental values[142,143]) and results of calculations of $(114)_2$ dimer [two points were obtained using two different computational methods, 4*c*-DFT[141] and REC CCSD(T)[77]].

chemical bonding. The $D_e(M_2)$ values were shown to correlate with the sublimation enthalpies $\Delta H_{sub}(M)$ (see Fig. 21); this was used to obtain the $\Delta H_{sub}(114)$ value using the calculated atomization energy $D_e[(114)_2]$; $\Delta H_{sub}(114) = 1.0 \pm 0.2$ eV.

b. Intermetallic systems

The electronic structure calculations of diatomic molecules MM′ (M = Ge, Sn, Pb, element 114; and M′ = Ni, Pb, Pt, Cu, Ag and Au) were performed by the 4*c*-DFT method.[141] It was shown that the chemical bonds formed by element 114 with Group 10 and 11 metal atoms are much weaker than those formed by lead. A Mulliken population analysis of 114Au showed that both the $7p_{1/2}(114)$ and $7p_{3/2}(114)$ AOs overlap with the 5d(Au) AOs. The type of bonding in 114Au should be similar to that in 112Au, although D_e(114Au) is about 0.2 eV higher than D_e(112Au). Among all metals considered, the bonding should be the strongest with Pt and the weakest with Ag and Ni.

The parameters D_e and R_e of MAu (M = Ge, Sn, Pb, element 114) are plotted *vs.* Z(M) in Fig. 22. The D_e(MAu)-*vs.*-Z plot obeys the same pattern as the $D_e(M_2)$-*vs.*-Z plot in Fig. 21. Assuming that the correlation between the atomization energies D_e(MAu) and the enthalpies of adsorption on gold, $-\Delta H_{ads}(M)$, is similar to the $D_e(M_2)$-*vs.*-$\Delta H_{sub}(M)$ correlation shown in Fig. 21, $-\Delta H_{ads}(114) = 0.95$ eV was obtained using the measured $-\Delta H_{ads}$(Pb). This result is in very good agreement with the value $-\Delta H_{ads}(114) = 0.97$ eV obtained from semiempirical calculations.[144]

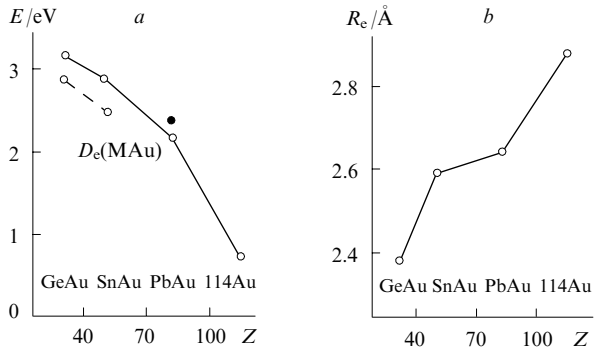


Figure 22. Dissociation energies (*a*) (solid lines represent the results of calculations [141] and the dashed line represents experimental data) and calculated bond lengths (*b*) in MAu (M = Ge, Sn, Pb, element 114) dimers.[18]
The filled circle denotes the measured $-\Delta H_{ads}$ of Pb on gold.

The interaction of Pb and element 114 with large gold clusters (up to 120 atoms) simulating the Au(100) and Au(111) surfaces was calculated by the 4*c*-DFT method.[131] The results obtained for the $M-Au_n$ ($n = 120$) systems suggest that element 114 is bound to gold about 1.3 eV weaker than Pb. A comparison with the Group 12 elements shows that the bonding to gold should increase in the following order:

$$112 < Hg < 114 \ll Pb,$$

as was obtained for the diatomic molecules MAu. Thus, in the gas thermochromatography experiments, element 114 should be adsorbed on gold detectors at the very beginning of the column, similarly to mercury.

c. Other compounds

Weaker involvement of the $7p_{1/2}$-electrons of element 114 in chemical bonding as compared with the lighter homologues in Group 14 was also demonstrated by calculations of other molecular systems. Among the atomization energies of Group 14 element hydrides, D_e(114H) is the smallest [59,77] and decreases by about 2 eV due to spin-orbit coupling.[57–59,77] The influence of the spin-orbit coupling on R_e is relatively small due to the contribution of both the contracted $7p_{1/2}$ and expanded $7p_{3/2}$ AOs. This is also obviously the reason why R_e(114H) = 1.96 Å is larger than R_e(PbH) = 1.88 Å. According to RECP CCSD(T) calculations [62] of PbH^+ and $114H^+$, the binding energy of the latter molecule is 0.48 eV lower, although the 114–H bond is 0.18 Å shorter. The CAS-SCF/SOCI RECP calculations of $114H_2$ demonstrated a breakdown of the conventional singlet (X^1A_1) and triplet ($^3B_1$) states due to large relativistic effects including the spin-orbit splitting.[145] It was shown that the spin-orbit effects destabilize $114H_2$ by almost 2.6 eV.

The electronic structures of 114X (X = F, Cl, Br, I, O, O_2) were calculated using the 2*c*-RECP CCSD(T), 2*c*-DFT SO ZORA and 4*c*-BDF methods.[74,77] Trends in R_e and D_e of the halides and oxides of the elements from lead to element 114 were found to be similar to those obtained for corresponding hydrides. It was predicted that, in contrast to PbO_2 ($D_e = 5.60$ eV), $114O_2$ ($D_e = 1.64$ eV) should be thermodynamically unstable with respect to the decomposition to the metal atom and O_2.[103] Correspondingly, element 114 should not react with O_2 under experimental conditions.

The *ab initio* DF and PP calculations [41–43,50] of the decomposition reactions

$$MX_4 \longrightarrow MX_2 + X_2,$$

$$MX_2 \longrightarrow M + X_2$$

(M = Si, Ge, Sn, Pb, 114; X = H, F, Cl)

confirmed a decrease in the stability of the 4+ oxidation state in agreement with earlier works (see, *e.g.*, Ref. 3). The instability was shown to be a relativistic effect. The possibility for a hexafluoride anion $114F_6^{2-}$ to exist was suggested.[42]

6. Elements 115–118

The chemical properties of the elements 115 and 116 have been poorly studied so far, although they are expected to be very interesting due to strong spin-orbit effects on the 7p AOs. The results of the early studies based on extrapolation of the properties and on atomic DF calculations are generalized in Ref. 3.

The results of the 4*c*-BDF and SO ZORA calculations of 115H and $(115)_2$ are in good agreement.[74,138] The 0_{g+} ground state was found for both Bi_2 and $(115)_2$. The 115 dimer was found to be weaker bound than Bi_2, namely, $D_e(115_2) = 0.83$ eV and $R_e = 3.08$ Å, while $D_e(Bi_2) = 2.45$ eV and $R_e = 2.69$ Å. The bonding in $(115)_2$ should also be stronger than in $(113)_2$ and $(114)_2$.

The RECP and BDF calculations [57,59,77] revealed that D_e(PoH) > D_e(116H) and R_e(PoH) < R_e(116H). Relativistic effects cause R_e(116H) to increase and D_e(116H) to decrease. The RECP method was also applied to the hydride $116H_2$.[63] It was found that the spin-orbit interaction leads

to elongation of the 116–H bond and to a significant increase in the H–116–H bond angle compared to the H–Po–H bond angle in PoH_2. It was assumed that the result is a rehybridization of the valence 7p AO with a 'supervalent' 8s AO of element 116.

The assumption of reduced stability of the 4+ oxidation state of element 116 was supported by the estimates of the formation enthalpies of MX_2 and MX_4 (M = Po, 116; X = F, Cl, Br, I, SO_4^{2-}, CO_3^{2-}, NO_3^-, PO_4^{3-}) obtained using the results of the atomic MCDF calculations.[146] The chemistry of element 116 is expected to be mainly cationic, namely, the ease of formation of divalent compounds should approach that of formation of Be or Mn divalent compounds, while tetravalent compounds should be formed with the most electronegative atoms (*e.g.*, with fluorine, $116F_4$).

The DF and RECP calculations showed that element 117 should form H117 by analogy with other Group 17 element halides.[38, 58] The bond in H117 should be weaker than in the other HM compounds (M = Group 17 elements) in line with a decreasing trend in Group 17; $R_e(H117) > R_e(HAt)$, also in line with the trend observed. These trends are due to a decreasing contribution of the $np_{1/2}$-AO with increasing Z(M) in the group.

Similarly to the lighter homologues, element 117 should also form a dimmer $(117)_2$.[147] The bonding in $(117)_2$ is predicted to be of mainly π character. Calculations also predict the existence of 117Cl with a single π-bond lengthened due to the spin-orbit effects.[148] The IF, AtF and 117F molecules were also considered at the DC and RECP + HF/MP2/CCSD/CCSD(T) levels of theory.[102] D_e(117F) is expected to be the largest among those of the Group 17 element fluorides. It was found that, unlike the D_e values of the other Group 17 element fluorides, the D_e(117F) value is increased by 0.1 eV due to the spin-orbit effects. The SO effects are opposite on the spectroscopic constants of 113F and 117F. According to PP calculations,[43] the D_{3h} geometry is inappropriate for the $117F_3$ molecule, in contrast to the astatine (sixth-row element) compound; this again indicates that the VSERP theory is inapplicable to SHE.

The chemical properties of element 118 should be interesting due to the very large spin-orbit splitting of the 7p AO (11.8 eV).[19] The destabilization of four $7p_{3/2}$-electrons suggests that element 118 should be relatively reactive, in line with an increasing trend in the reactivity of Group 18 elements. It should also be the most electronegative element among the noble gases due to the relativistic stabilization of the 8s AO. The DCB CCSD + QED calculations gave an electron affinity of 0.058 eV for element 118.[22] The polarizability and atomic radius obtained from DC CCSD(T) calculations are $\alpha(118) = 46.3$ a.u. and $AR(118) = 4.55$ a.u., being the largest among the Group 18 elements, whereas the ionization potential $IP(118) = 8.92$ eV is the smallest.[95] In addition to general trends in the periodic table, these extreme values for Group 18 reflect the relativistic expansion of the $7p_{3/2}$ AO.

Using the calculated atomic properties and the adsorption model [see Eqn (6)], the van der Waals coefficients (C_3) and the enthalpies of adsorption of the Group 18 elements on noble metal and inert surfaces, such as quartz, ice, Teflon and graphite (Fig. 23) were calculated.[85] It was shown that the C_3 coefficients steadily increase on going from neon to element 118, whereas the increase in $-\Delta H_{ads}$ on going from Ne to Rn does not continue to element 118; the large atomic radius of element 118 is responsible for the

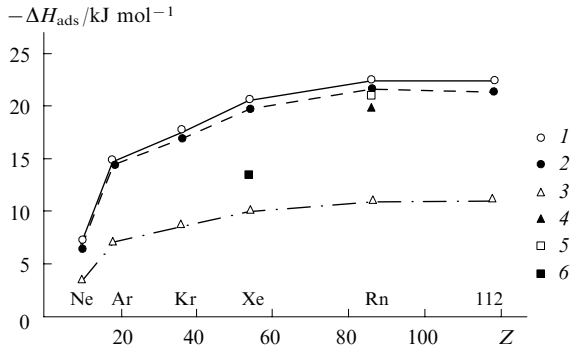


Figure 23. Calculated adsorption enthalpies of noble gas atoms on quartz (*1*), ice (*2*) and Teflon (*3*).[95]
Shown are the experimental data for adsorption of radon on quartz (*4*) (B Eichler, private communication) and ice[125] (*5*) and for adsorption of xenon on ice[149] (*6*).

equal ΔH_{ads} values of 118 and radon. Therefore, the separation of element 118 and radon by adsorption on these types of surfaces is expected to be difficult. A possible candidate for separation of the two elements is charcoal; verification of this assumption requires further studies.

The RECP calculations of the reactions

$$M + F_2 \longrightarrow MF_2,$$

$$MF_2 + F_2 \longrightarrow MF_4$$

(M = Xe, Rn, element 118)

revealed an increasing stability of the Group 18 element fluorides.[49, 55] It was shown that the spin-orbit effects considerably stabilize $118F_4$ (by about 2 eV), although they elongate R_e by 0.05 Å. Thus, the trends in increasing R_e and D_e are continued with element 118. Also, the following trends in stability of the fluorides were established:

$$RnF_2 < HgF_2 < PbF_2,$$

$$112F_2 < 114F_2 < 118F_2.$$

The influence of the spin-orbit coupling on the geometry of MF_4 was investigated by the RECP-SOCI[60, 62, 150] and RECP CCSD methods.[55] It was shown that the D_{4h} geometric configuration typical of XeF_4 and RnF_4 becomes unstable for $118F_4$. A T_d configuration of $118F_4$ is 0.25 eV (Refs 60, 61 and 150) or 0.17 eV (Refs 49 and 55) more stable than the D_{4h} configuration. The reason for this unusual geometry is the availability of only the stereochemically active $7p_{3/2}$ electrons for bonding. This is yet another example of the inapplicability of the VSERP theory to SHE. An important assumption was made that the fluorides of element 118 will most probably be ionic rather than covalent, as in the case of Xe. This prediction may be useful for the design of future gas-phase chromatography experiments.

The RECP calculations[58] of 118H showed the van der Waals bond in this compound to be stabilized by about 2.0 MeV by the spin-orbit effects with $\Delta R_e(SO) = -0.019$ Å. The following trends in stability of hydrides were predicted:

$$RnH \ll HgH < PbH,$$

$$118H \ll 114H < 112H.$$

The RECP calculations[62] of singly charged ions gave $D_e(RnH^+) > D_e(118H^+)$ and $R_e(RnH^+) < R_e(118H^+)$.

7. Elements with $Z > 118$

A very long, unprecedented series of transition elements begins with element 122. These elements were called 'superactinides'.[151,152] A number of theoretical calculations of the ground-state electronic configurations of these elements were performed (see review[3] and Ref. 86). It is expected that four ($8p_{1/2}$, $7d_{3/2}$, $6f_{5/2}$ and $5g_{7/2}$) rather than two electron shells will be simultaneously filled in the early superactinides. These open shells, together with the 8s electrons, will determine the chemical properties of these elements. According to the DS calculations,[3] the g-electrons first appear in element 125; however, relativistic DFT calculations with QED corrections (Breit interaction)[86] revealed the first appearance of g electrons in element 126. It was also shown that the QED corrections are important for studying electronic configurations of SHE.

Due to strong relativistic effects, the chemical properties of superactinides will be significantly different from those of SHE. However, even with no relativistic effects included, their properties would also be different due to very large orbital effects. At present, almost no MO studies of compounds of these elements are available. Accurate prediction of the properties of particular compounds will be a challenge. QED-corrected relativistic calculations may be needed to reach the desired accuracy.

8. Predictions of the volatility of transactinides and their compounds

The predicted trends in volatility of the heaviest elements and their compounds are compared with experimental observations in Table 5. One can see that all the trends predicted for the Group 4–8 and Group 12 elements were confirmed by the experiments. The predictions for element 114 are still awaiting an experimental verification.

VI. Complexation and extraction

A number of experiments on liquid-phase extraction and chromatographic separation of Rf, Db and Sg and their homologues from HF, HCl and mixed acid solutions were reported (see references cited in Refs 7–11, 13 and 17). These experiments demonstrated a basic similarity in the extraction behaviour of transactinides and their lighter homologues, although revealed a number of controversies. Many theoretical works[156–163] were devoted to prediction of complexation and the extraction behaviour of these elements. They were based on the results of 4*c*-DFT calculations of the electron density distribution in the species participating in chemical equilibria. To calculate the change in the Gibbs free energy of a complexation reaction, a model was used, which treats ΔG as the sum of the electrostatic, covalent, and entropy terms. Using this model, the hydrolysis and complexation constants were predicted for a large number of aqueous compounds of Rf, Db, Sg and Hs and their lighter homologues in Groups 4, 5, 6 and 8.[156–163] The results of the calculations showed that the predominant contribution to ΔG comes from the change in the electrostatic metal–ligand interaction energy (ΔE_C).

Consider a stepwise complexation of Group 4 elements (Zr, Hf, Rf) in H_2SO_4 solutions as an example. The relative changes in the Gibbs free energy of formation of $M(SO_4)_2(H_2O)_4$, $M(SO_4)_3(H_2O)_2^{2-}$ and $M(SO_4)_4^{4-}$ (M = Zr, Hf, Rf) from hydrated and partially hydrolyzed cations were calculated[157] by the 4*c*-DFT method. The geometries of two of these complexes are shown in Fig. 24. The calculated ΔE_C values and trends for one type of the complexation reactions starting from the hydrated species $M(H_2O)_8^{4+}$ are given in Table 6. The ΔE_C values for the complexation reactions starting from hydrolyzed complexes

$$MOH(H_2O)_7^{3+} \rightleftharpoons M(SO_4)_n(H_2O)_{8-2n}$$

were obtained analogously.

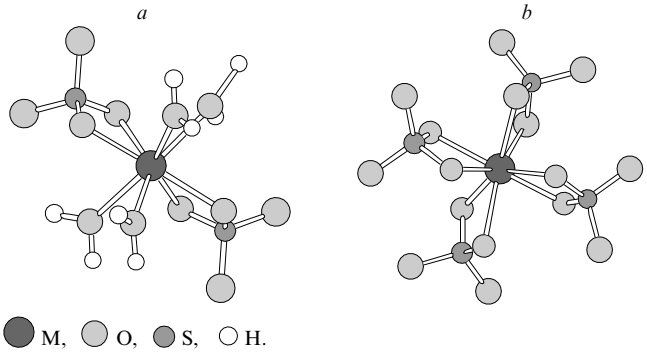


Figure 24. Structures of $M(SO_4)_2(H_2O)_4$ (*a*) and $M(SO_4)_4^{4-}$ (*b*) complexes (M = Zr, Hf, Rf).[157]

The results obtained revealed the same trend in complexation (Zr > Hf ≫ Rf) as that found for the former reaction type (see Table 6). The log K_d values (K_d is the distribution cooefficient) for extraction of Zr, Hf and Rf by amines are shown in Fig. 25.

Experiments on the extraction of Zr, Hf and Rf from H_2SO_4 solutions by amines confirmed the predicted trend in complexation

$$Zr > Hf \gg Rf$$

and gave the K_d(Rf) values close to the predicted ones.[164]

Table 5. Trends in volatility of transactinide compounds and their lighter homologues in groups of the periodic table.

Group	Compounds	Theoretical prediction	Ref.	Experiment	Ref.
4	MCl_4, MBr_4	Hf < Rf	106	Hf < Rf	154
5	ML_5 (L = Cl, Br)	Nb < Ta < Db	153	(DbO_3Br)	155
		$DbCl_5 > DbOCl_3$	153	$DbCl_5 > DbOCl_3$	155
6	MO_2Cl_2	Mo > W > Sg	107	Mo > W > Sg	109, 110
7	MO_3Cl	Tc > Re > Bh	113	Tc > Re > Bh	117
8	MO_4	Ru < Os > Hs	116	Os > Hs	118
12	M	Hg < 112	126–129	Hg < 112	132
14	M	Pb ≪ 114 < 112	131	–	–

Table 6. Coulomb part of changes in the Gibbs free energy ($-\Delta E_C$/eV) of the complexation reactions.[157]

Reaction	Zr	Hf	Rf	Trend
$M(H_2O)_8^{4+} \rightleftharpoons M(SO_4)_2(H_2O)_4$	35.72	35.84	33.60	Hf > Zr ≫ Rf
$M(H_2O)_8^{4+} \rightleftharpoons M(SO_4)_3(H_2O)_2^{2-}$	42.43	42.43	39.37	Zr = Hf ≫ Rf
$M(H_2O)_8^{4+} \rightleftharpoons M(SO_4)_4^{4-}$	45.14	45.02	41.38	Zr > Hf ≫ Rf
$M(H_2O)_8^{4+} \rightleftharpoons R_4M(SO_4)_4$	41.04	40.78	37.65	Zr > Hf ≫ Rf

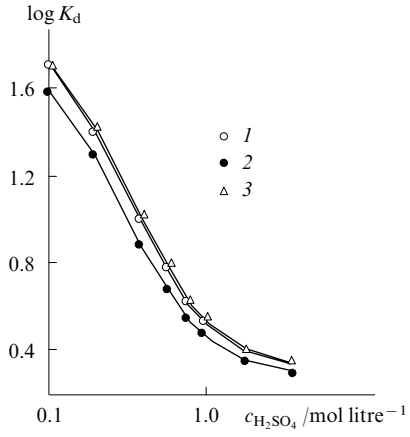


Figure 25. Predicted logK_d values for extraction of Hf (*1*) and Rf (*2*) by amines and experimental data for Zr (*3*).[145]

The predicted trends in hydrolysis, complexation and extraction of the complexes of transactinides and their homologues and the available experimental results have been analyzed in a review.[17] Almost all predictions for SHE were confirmed experimentally, although some of them are still to be confirmed (*e.g.*, the case of Sg in HF solutions).

VII. Conclusion

Numerous calculations of the atomic and molecular properties of transactinides and their homologues including the most accurate DCB CCSD(T) calculations have been performed as yet. Electronic configurations necessary for the determination of position of particular elements in the periodic table were calculated with a very high accuracy.

Accurate ionization potentials, electron affinities and energies of electronic transitions are also available and can be used to assess the similarity between the SHE and their lighter homologues in groups of the periodic table.

The most valuable information on the molecular properties of chemically interesting compounds was obtained using the 4*c*-DFT and RECP/PP CCSD(T) methods, which proved to be complimentary, both conceptually and quantitatively. Their combination is obviously the best way to predict the properties of SHE. Calculations using these methods allowed one to establish important trends in the chemical bonding, stabilities of oxidation states, crystal field and spin-orbit effects, complexing ability, *etc.* on going from light to heavier elements in the periodic table and to assess how the relativistic and correlation effects influence these properties.

It was shown that the transactinides are in essence homologues of lighter related elements in groups of the periodic table, although their properties may be rather different due to large relativistic effects. This is also the reason for changes in trends in the atomic and molecular properties on going to heavier elements. Thus, straightforward extrapolations of the properties in groups of the periodic table may result in erroneous predictions. Relativistic calculations proved to be the most reliable tool in predicting the outcome of the gas-phase and aqueous phase experiments with Rf, Db, Sg, Bh, Hs and element 112. The synergism between theoretical and experimental research in the last decades led to a better insight into the chemistry of these exotic elements.

In spite of rich information collected so far, a number of issues are still to be clarified. Research on the chemically investigated elements requires more detailed theoretical and experimental studies. New compounds of such elements, *e.g.*, seaborgium carbonyls or organohassium compounds should be synthesized and investigated. As to the elements not studied as yet (*e.g.*, Mt, Ds, Rg, elements 115–118), isotopes suitable for chemical research should be found. Theoretical chemists will have to solve a number of problems concerning prediction of the experimental behaviour of these elements in the chemical separation experiments.

Investigations of the chemical properties of elements with $Z > 118$ is a matter of future. These studies will be even more exciting than those performed so far, because similarity between these elements and their lighter homologues will be even less pronounced. Further methodical developments in the relativistic quantum theory, *e.g.*, the inclusion of the QED effects on a SCF basis, may be needed to achieve a required accuracy of calculations.

References

1. S Hofmann, G Münzenberg *Rev. Mod. Phys.* **72** 733 (2000)
2. Yu Oganessian *J. Phys. G: Nucl. Part. Phys.* **34** R165 (2007)
3. B Fricke *Struct. Bond.* **21** 89 (1975)
4. *The Chemistry of the Superheavy Elements* (Ed. M.Schädel) (Dordrecht: Kluwer Academic, 2003)
5. H W Gäggeler, A Türler, in *The Chemistry of the Superheavy Elements* (Ed. M Schädel) (Dordrecht: Kluwer Academic, 2003) p. 237
6. A Türler, K E Gregorich, in *The Chemistry of the Superheavy Elements* (Ed. M Schädel) (Dordrecht: Kluwer Academic, 2003) p. 117
7. D C Hoffman *Chem. Eng. News* **72** (18) 24 (1994)
8. D C Hoffman *J. Chem. Ed.* **76** 331 (1999)
9. J V Kratz, in *The Chemistry of the Superheavy Elements* (Ed. M Schädel) (Dordrecht: Kluwer Academic, 2003) p. 104
10. J Kratz, in *Handbook of Nuclear Chemistry* (Eds S Nagy, Z Klencsar) (Dordrecht: Kluwer Academic, 2003) p. 323
11. M Schädel *Angew. Chem., Int. Ed.* **45** 368 (2006)
12. V Pershina *Chem. Rev.* **96** 1977 (1996)
13. V Pershina, J V Kratz, in *Relativistic Effects in Heavy-Element Chemistry and Physics* (Ed. B A Hess) (West Sussex: Wiley, 1997) p. 219
14. P Schwerdtfeger, M Seth, in *Encyclopedia on Calculational Chemistry* Vol. 4 (New York: Wiley, 1998) p. 2480
15. V Pershina, in *Relativistic Electronic Structure Theory* Pt. 2 (Ed. P Schwerdtfeger) (Amsterdam: Elsevier, 2004) p. 1
16. V Pershina, in *The Chemistry of the Superheavy Elements* (Ed. M Schädel) (Dordrecht: Kluwer Academic, 2003) p. 31
17. D C Hoffman, D M Lee, V Pershina, in *The Chemistry of the Actinide and Transactinide Elements* Ch. 14 (3rd Ed.) (Eds L R Morss, N M Edelstein, J Fuger) (Dordrecht: Springer, 2006) p. 1652
18. V Pershina, in *Relativistic Methods for Chemists* (Eds M Barysz, Y Ishikawa) (London: Springer, in the press)

19. J P Desclaux *At. Data Nucl. Data Tables* **12** 311 (1973)
20. E Eliav, S Shmulyian, U Kaldor, Y Ishikawa *J. Chem. Phys.* **109** 3954 (1998)
21. N Gaston, P Schwerdtfeger, W Nazarewicz *Phys. Rev. A* **66** 062505 (2002)
22. I Goidenko, L Labsowsky, E Eliav, U Kaldor, P Pyykkl *Phys. Rev. A* **67** 020102(R) (2003)
23. U Kaldor, E Eliav, A Landau, in *Relativistic Electronic Structure Theory* Pt. 1 (Ed. P Schwerdtfeger) (Amsterdam: Elsevier, 2004) p. 81
24. DIRAC package Dirac, a relativistic *ab initio* electronic structure programme Release DIRAC04.0 (2004); http://dirac.chem.sdu.dk
25. J P Desclaux *Comp. Phys. Commun.* **9** 31 (1975)
26. I P Grant *J. Phys. B* **19** 3187 (1986)
27. B Fricke, E Johnson, G M Rivera *Radiochim. Acta* **62** 17 (1993)
28. E Johnson, V Pershina, B Fricke *J. Phys. Chem.* **103** 8458 (1999)
29. E Johnson, B Fricke, T Jacob, C Z Dong, S Fritzsche, V Pershina *J. Phys. Chem.* **116** 1862 (2002)
30. Y J Yu, J G Li, C Z Dong, X B Ding, S Fritsche, B Fricke *Eur. Phys. J. D* **44** 51 (2007)
31. Y J Yu, C Z Dong, J G Li, B Fricke *J. Chem. Phys.* **128** 124316 (2008)
32. V I Nefedov, M B Trzhaskovskaya, V G Yarzhemskii *Dokl. Phys. Chem.* **408** 149 (2006)
33. K Balasubramanian *Chem. Phys. Lett.* **341** 601 (2001)
34. K Balasubramanian *Chem. Phys. Lett.* **351** 161 (2002)
35. L Visscher, in *Relativistic Electronic Structure Theory* Pt. 1 (Ed. P Schwerdtfeger) (Amsterdam: Elsevier, 2004) p. 291
36. T Saue, in *Relativistic Electronic Structure Theory* Pt. 1 (Ed. P Schwerdtfeger) (Amsterdam: Elsevier, 2004) p. 332
37. C P Wood, N C Pyper *Chem. Phys. Lett.* **84** 614 (1981)
38. T Saue, K Faegri, O Gropen *Chem. Phys. Lett.* **263** 360 (1996)
39. M Seth, P Schwerdtfeger, M Dolg, K Faegri, B A Hess, U Kaldor *Chem. Phys. Lett.* **250** 461 (1996)
40. M Seth, P Schwerdtfeger *Chem. Phys. Lett.* **318** 314 (2000)
41. K Faegri, T Saue *J. Chem. Phys.* **115** 2456 (2001)
42. M Seth, K Faegri, P Schwerdtfeger *Angew. Chem., Int. Ed.* **37** 2493 (1998)
43. P Schwerdtfeger, M Seth *J. Nucl. Radiochem. Sci.* **3** 133 (2002)
44. M Seth, P Schwerdtfeger, K Faegri *J. Chem. Phys.* **111** 6422 (1999)
45. G L Malli, J Styszynski *J. Chem. Phys.* **109** 4448 (1998)
46. G Malli *J. Chem. Phys.* **116** 5476 (2002)
47. G Malli *J. Chem. Phys.* **117** 10441 (2002)
48. M Dolg, in *Relativistic Electronic Structure Theory* Pt. 1 (Ed. P Schwerdtfeger) (Amsterdam: Elsevier, 2004) p. 793
49. Y S Lee, in *Relativistic Electronic Structure Theory* Pt. 1 (Ed. P Schwerdtfeger) (Amsterdam: Elsevier, 2004) p. 352
50. M Seth Ph.D. Thesis, University of Auckland, Auckland, 1998
51. M Seth, M Dolg, P Fulde, P Schwerdtfeger *J. Am. Chem. Soc.* **117** 6597 (1995)
52. M Seth, P Schwerdtfeger, M Dolg *J. Chem. Phys.* **106** 3623 (1997)
53. M Seth, F Cooke, P Schwerdtfeger, J-L Heully, M Pelissier *J. Chem. Phys.* **109** 3935 (1998)
54. Y K Han, S-K Son, Y J Choi, Y S Lee *J. Phys. Chem. A* **103** 9109 (1999)
55. Y K Han, Y S Lee *J. Phys. Chem. A* **103** 1104 (1999)
56. Y K Han, C Bae, Y S Lee *J. Chem. Phys.* **110** 8986 (1999)
57. Y-K Han, C Bae, S-K Son, Y S Lee *J. Chem. Phys.* **112** 2684 (2000)
58. Y J Choi, Y K Han, Y S Lee *J. Chem. Phys.* **115** 3448 (2001)
59. C S Nash, B E Bursten *J. Phys. Chem. A* **103** 632 (1999)
60. C S Nash, B E Bursten *J. Phys. Chem. A* **103** 402 (1999)
61. C S Nash, B E Bursten *Angew. Chem., Int. Ed.* **38** 151 (1999)
62. C S Nash *J. Phys. Chem. A* **109** 3493 (2005)
63. C S Nash, W W Crockett *J. Phys. Chem. A* **110** 4619 (2006)
64. K Balasubramanian *Chem. Phys. Lett.* **361** 397 (2002)
65. C S Nash, B E Bursten, W C Ermler *J. Chem. Phys.* **106** 5153 (1997)
66. N S Mosyagin, A N Petrov, A V Titov, I I Tupitsyn, in *Recent Advances in the Theory of Chemical and Physical Systems* (Berlin: Springer, 2006) p. 229
67. W Kohn, A D Becke, R G Parr *J. Phys. Chem.* **100** 12974 (1996)
68. E Engel, in *Relativistic Electronic Structure Theory* Pt. 1 (Ed. P Schwerdtfeger) (Amsterdam: Elsevier, 2004) p. 523
69. A Rosen, D E Ellis *J. Chem. Phys.* **62** 3039 (1975)
70. A Rosen *Adv. Quantum. Chem.* **29** 1 (1997)
71. T Bastug, W-D Sepp, D Kolb, B Fricke, G te Velde, E J Baerends *J. Phys. B* **28** 2325 (1995)
72. J Anton, B Fricke, E Engel *Phys. Rev. A* **69** 012505 (2004)
73. T Jacob, D Geschke, S Fritzsche, W-D Sepp, B Fricke, J Anton, S Varga *Surf. Sci.* **486** 194 (2001)
74. C van Wüllen, in *Relativistic Electronic Structure Theory* Pt. 2 (Ed. P Schwerdtfeger) (Amsterdam: Elsevier, 2004) p. 598
75. W Liu, G Hong, D Dai, L Li, M Dolg *Theor. Chem. Acc.* **96** 75 (1997)
76. W Liu, Ch van Wüllen *J. Chem. Phys.* **110** 3730 (1999)
77. W Liu, Ch van Wüllen, Y K Han, Y J Choi, Y S Lee *Adv. Quantum. Chem.* **39** 325 (2001)
78. M Mayer, S Krüger, N Rösch *J. Chem. Phys.* **115** 4411 (2001)
79. B A Hess *Phys. Rev. A* **33** 3742 (1986)
80. E Eliav, U Kaldor, Y Ishikawa *Phys. Rev. A* **52** 291 (1995)
81. J P Desclaux, B Fricke *J. Phys.* **41** 943 (1980)
82. V A Glebov, L Kasztura, V S Nefedov, B L Zhuikov *Radiochim. Acta* **46** 117 (1989)
83. E Johnson, B Fricke, O L Keller Jr, C W Nestor Jr, T C Ticker *J. Chem. Phys.* **93** 8041 (1990)
84. E Eliav, U Kaldor, Y Ishikawa *Phys. Rev. Lett.* **74** 1079 (1995)
85. E Eliav, A Landau, Y Ishikawa, U Kaldor *J. Phys. B* **3** 1693 (2002)
86. K Umemoto, S Saito *J. Phys. Soc. Jpn.* **65** 3175 (1996)
87. N C Pyper, I P Grant *Proc. R. Soc. London, Ser. A* **376** 483 (1981)
88. E Eliav, U Kaldor, P Schwerdtfeger, B A Hess, Y Ishikawa *Phys. Rev. Lett.* **73** 3203 (1994)
89. E Eliav, U Kaldor, Y Ishikawa *Phys. Rev. A* **52** 2765 (1995)
90. E Eliav, U Kaldor, Y Ishikawa, M Seth, P Pyykkl *Phys. Rev. A* **53** 3926 (1996)
91. A Landau, E Eliav, Y Ishikawa, U Kaldor *J. Chem. Phys.* **114** 2977 (2001)
92. E Eliav, U Kaldor, Y Ishikawa *Mol. Phys.* **94** 181 (1998)
93. C E Moore *Atomic Energy Levels (Natl. Stand. Ref. Data Ser.)* (Washington, DC: Natl. Bur. Stand., 1971)
94. E Eliav, U Kaldor, Y Ishikawa, P Pyykkö *Phys. Rev. Lett.* **77** 5350 (1996)
95. V Pershina, A Borschevsky, E Eliav, U Kaldor *J. Chem. Phys.* **129** 144106 (2008)
96. I Lim, M Pernpointer, M Seth, P Schwerdtfeger *Phys. Rev. A* **60** 2822 (1999)
97. I S Lim, P Schwerdtfeger, B Metz, H Stoll, *J. Chem. Phys.* **122** 194103 (2005)
98. A Landau, E Eliav, Y Ishikava, U Kaldor *J. Chem. Phys.* **115** 2389 (2001)
99. C Thierfeld, P Schwerdtfeger, F P Hessberger, S Hofmann *Eur. Phys. J. A* **36** 227 (2008)
100. R D Shannon *Acta Crystallogr., Sect. A* **32** 751 (1976)
101. P Pyykkö, M Atsumi *Chem. – Eur. J.* **15** 186 (2009)
102. P Pyykkö, S Riedel, M Patzsche *Chem. – Eur. J.* **11** 3511 (2005)
103. V Pershina, A Borschevsky, E Eliav, U Kaldor *J. Chem. Phys.* **128** 024707 (2008)
104. V Pershina, A Borschevsky, E Eliav, U Kaldor *J. Phys. Chem. A* **112** 13712 (2008)
105. V Pershina, B Fricke *J. Chem. Phys.* **99** 9720 (1993)
106. V Pershina, B Fricke, in *Heavy Elements and Related New Phenomena* (Eds W Greiner, R K Gupta) (Singapore: World Scientific, 1999) p. 194
107. V Pershina, B Fricke *J. Phys. Chem.* **99** 144 (1995)
108. V Pershina, B Fricke *J. Phys. Chem.* **100** 8748 (1996)
109. M Schädel, W Brüchle, R Dressler, B Eichler, H W Gäggeler, R Günther, K E Gregorich, D C Hoffman, S Hübener, D T Jost, J V Kratz, W Paulus, D Schumann, S Timokhin, N Trautmann, A Türler, G Wirth, A B Yakushev *Nature (London)* **388** 55 (1997)

110. A Türler, W Brüchle, R Dressler, B Eichler, R Eichler, H W Gäggeler, M Gärtner, J-P Glatz, K E Gregorich, S Hübener, D T Jost, V Y Lebedev, V Pershina, M Schädel, S Taut, N Timokhin, N Trautmann, A Vahle, A B Yakushev *Angew. Chem., Int. Ed.* **38** 2212 (1999)
111. C S Nash, B E Bursten *New J. Chem.* **19** 669 (1995)
112. S Varga, B Fricke, M Hirata, T Bastug, V Pershina, S Fritzsche *J. Phys. Chem.* **104** 6495 (2000)
113. V Pershina, T Bastug *J. Chem. Phys.* **113** 1441 (2000)
114. V Pershina, T Bastug, B Fricke, S Varga *J. Chem. Phys.* **115** 1 (2001)
115. V Pershina, T Bastug, B Fricke *J. Chem. Phys.* **122** 124301 (2005)
116. V Pershina, J Anton, T Jacob *Phys. Rev. A* **78** 032518 (2008)
117. R Eichler, W Brüchle, R Dressler, Ch E Düllman, B Eichler, H W Gäggeler, K E Gregorich, D C Hoffman, S Hübener, D T Jost, U W Kirbach, C A Laue, V M Lavanchy, H Nitsche, J B Patin, D Piguet, M Schädel, D A Shaughnessy, D A Strellis, S Taut, L Tobler, Y S Tsyganov, A Türler, A Vahle, P A Wilk, A B Yakushev *Nature (London)* **407** 63 (2000)
118. Ch E Düllmann, W Brüchle, R Dressler, K Eberhardt, B Eichler, R Eichler, H W Gäggeler, T N Ginter, F Glaus, K Gregorich, D C Hoffman, E Jäger, D T Jost, U W Kirbach, D E Lee, H Nitsche, J B Patin, V Pershina, D Piguet, Z Qin, M Schädel, B Schausten, E Schimpf, H-J Schött, S Soverna, R Sudowe, P Thörle, S N , Timokhin, N Trautmann, A Türler, A Vahle, G Wirth, A B Yakushev, P M Zielinski *Nature (London)* **418** 859 (2002)
119. M Filatov, D Cremer *J. Chem. Phys.* **119** 1412 (2003)
120. J Anton, B Fricke, P Schwerdtfeger *Chem. Phys.* **311** 97 (2005)
121. K S Pitzer *J. Chem. Phys.* **63** 1032 (1975)
122. V Pershina, T Bastug *Chem. Phys.* **311** 139 (2005)
123. P Schwerdtfeger, J Li, P Pyykkö *Theor. Chim. Acta* **87** 313 (1994)
124. N Gaston, I Opahle, H W Gäggeler, P Schwerdtfeger *Angew. Chem., Int. Ed.* **46** 1663 (2007)
125. S Soverna, R Dressler, C E Düllmann, B Eichler, R Eichler, H W Gäggeler, F Haenssler, J P Niklaus, D Piguet, Z Qin, A Türler, A Yakushev *Radiochim. Acta* **93** 1 (2005)
126. V Pershina, T Bastug, B Fricke, T Jacob, S Varga *Chem. Phys. Lett.* **365** 176 (2002)
127. C Sarpe-Tudoran, V Pershina, B Fricke, J Anton, W-D Sepp, T Jacob *Eur. Phys. J. D* **24** 65 (2003)
128. V Pershina, T Bastug, C Sarpe-Tudoran, J Anton, B Fricke *Nucl. Phys. A* **734** 200 (2004)
129. C Sarpe-Tudoran, B Fricke, J Anton, V Pershina *J. Chem. Phys.* **126** 174702 (2007)
130. J P Niklaus, R Eichler, S Soverna, H W Gäggeler, L Tobler *PSI Annu. Rep.* 8 (2000)
131. V Pershina, J Anton, T Jacob *J. Chem. Phys.* **131** 084713 (2009)
132. R Eichler, N V Aksenov, A V Belozerov, G A Bozhikov, V I Chepigin, S N Dmitriev, R Dressler, H W Gäggeler, A V Gorshkov, M G Itkis, F Haenssler, A Laube, V Ya Lebedev, O N Malyshev, Yu Ts Oganessian, O V Petrushkin, D Piguet, A G Popeko, P Rasmussen, S V Shishkin, A A Serov, A V Shutov, A I Svirikhin, E E Tereshatov, G K Vostokin, M Wegrzecki, A V Yeremin *Angew. Chem., Int Ed.* **47** 3262 (2008)
133. E A Rykova, A Zeitsevskii, N S Nosyagin, T A Isaev, A V Titov *J. Chem. Phys.* **125** 241102 (2006)
134. N S Mosyagin, T A Isaev, A V Titov *J. Chem. Phys.* **124** 224302 (2006)
135. T Nakajima, K Hirao *Chem. Phys. Lett.* **329** 511 (2000)
136. *CRC Handbook of Chemistry and Physics* (86th Ed.) (Ed. D R Lide) ((Boca Raton, FL: CRC Press, 2005)
137. D Goeben, U Hohm *J. Phys. Chem.* **100** 7710 (1996)
138. W Liu, C van Wüllen, F Wang, L Li *J. Chem. Phys.* **116** 3626 (2002)
139. P Schwerdtfeger *J. Phys. Chem.* **100** 2968 (1996)
140. C Thierfelder, B Assadollahzadeh, P Schwerdtfeger, S Schäfer, R Schäfer *Phys. Rev. A* **78** 2968 (2008) 052506
141. V Pershina, J Anton, B Fricke *J. Chem. Phys.* **127** 134310 (2007)
142. K S Pitzer, K Balasubramanian *J. Phys. Chem.* **86** 3068 (1982)
143. M C Heaven, T A Miller, V E Bondybey *J. Phys. Chem.* **87** 2071 (1983)
144. H Rossbach, B Eichler *Akademie der Wissenschaft der DDR, Rossendorf, 1984* Report No ZFK-527
145. K Balasubramanian *J. Chem. Phys.* **117** 7426 (2002)
146. I P Grant, N C Pyper *Nature (London)* **265** 715 (1977)
147. L Visscher, K G Dyall *J. Chem. Phys.* **104** 9040 (1996)
148. G L Malli, in *Relativistic and Electron Correlation Effects in Molecules and Solids (NATO ASI Ser.)* Vol. 318 (New York: Plenum, 1994)
149. A P Graham, J P Toennies *J. Chem. Phys.* **118** 2879 (2003)
150. C S Nash, B E Bursten *Angew. Chem., Int. Ed.* **38** 151 (1999)
151. G T Seaborg, W D Loveland *The Elements beyond Uranium* (New York: Wiley, 1990)
152. G T Seaborg *J. Chem. Soc., Dalton Trans.* 760 (1996)
153. V Pershina, W-D Sepp, T Bastug, B Fricke, G V Ionova *J. Chem. Phys.* **97** 1123 (1992)
154. B Kadkhodayan, A Türler, K E Gregorich, P A Baisden, K R Czerwinski, B Eichler, H W Gäggeler, T M Hamilton, D T Jost, C D Kacher, A Kovacs, S A Kreek, M R Lane, M F Mohar, M P Neu, N J Stoyer, E R Sylwester, D M Lee, M J Nurmia, G T Seaborg, D C Hoffman *Radiochim. Acta* **72** 169 (1996)
155. A Türler *Radiochim. Acta* **72** 7 (1996)
156. V Pershina, D Trubert, C Le Naour, J V Kratz *Radiochim. Acta* **90** 869 (2002)
157. V Pershina, D Polakova, J P Omtvedt *Radiochim. Acta* **94** 407 (2006)
158. V Pershina *Radiochim. Acta* **80** 65 (1998)
159. V Pershina *Radiochim. Acta* **80** 75 (1998)
160. V Pershina, T Bastug *Radiochim. Acta* **84** 79 (1999)
161. V Pershina, J V Kratz *Inorg. Chem.* **40** 776 (2001)
162. V Pershina *Radiochim. Acta* **92** 455 (2004)
163. V Pershina *Radiochim. Acta* **93** 373 (2005)
164. J P Omtwedt, D Polyakova, J Alstad, T Bjornstad, C E Düllmann, C M Folden III, M A Garcia, J Gates, K E Gregorich, D C Hoffman, S L Nelson, H Nitsche, L Omtwedt, V Pershina, F Samadani, G Skarnemark, L Stavsetra, R Sudove, R E Wilson, L Zheng, P M Zielinski *Radiochim. Acta* (2010) (in the press)